Quaternary Science Reviews 192 (2018) 208–224

Contents lists available at ScienceDirect

Quaternary Science Reviews

journal homepage: www.elsevier.com/locate/quascirev

Seasonal variability in the abundance and stable carbon-isotopic composition of lipid biomarkers in suspended particulate matter from a stratified equatorial lake (Lake Chala, Kenya/Tanzania): Implications for the sedimentary record

L.G.J. van Bree [a, *], F. Peterse [a], M.T.J. van der Meer [b], J.J. Middelburg [a], A.M.D. Negash [a], W. De Crop [c], C. Cocquyt [c, d], J.J. Wieringa [e], D. Verschuren [c], J.S. Sinninghe Damsté [a, b]

[a] Utrecht University, Faculty of Geosciences, Department of Earth Sciences, Princetonlaan 8A, 3584 CD, Utrecht, The Netherlands
[b] NIOZ Royal Netherlands Institute for Sea Research, Department of Marine Microbiology and Biogeochemistry, Utrecht University, PO Box 59, 1790 AB, Den Burg, The Netherlands
[c] Ghent University, Limnology Unit, K.L. Ledeganckstraat 35, B-9000, Gent, Belgium
[d] Meise Botanic Garden, Nieuwelaan 38, B-1860, Meise, Belgium
[e] Naturalis Biodiversity Centre, P.O. Box 9517, 2300 RA, Leiden, The Netherlands

ARTICLE INFO

Article history:
Received 17 October 2017
Received in revised form
9 May 2018
Accepted 18 May 2018
Available online 6 June 2018

Keywords:
East Africa
Aquatic biomarkers
Organic geochemistry
Stable isotopes
Paleolimnology
Paleoclimatology

ABSTRACT

We studied the distribution and stable carbon-isotopic ($\delta^{13}C$) composition of various lipid biomarkers in suspended particulate matter (SPM) from the water column of Lake Chala, a permanently stratified crater lake in equatorial East Africa, to evaluate their capacity to reflect seasonality in water-column processes and associated changes in the lake's phytoplankton community. This lake has large seasonal variation in water-column dynamics (stratified during wet seasons and mixing during dry seasons) with associated phytoplankton succession. We analyzed lipid biomarkers in SPM collected monthly at 5 depths (0–80 m) from September 2013 to January 2015. Seasonal variation in total phytoplankton biovolume is strongly reflected in the concentration of phytadienes, a derivative of the general photosynthetic pigment chlorophyll. The wax and wane of several specific biomarker lipids between June and December 2014 reflect pronounced phytoplankton succession after deep mixing, starting with a long and sustained chlorophyte bloom (reflected by $C_{23:1}$, $C_{25:1}$ and $C_{27:1}$ *n*-alkenes, and C_{21} and C_{23} *n*-alkanes), followed by a peak in diatoms between July and October (loliolide and isololiolide), and then eustigmatophytes (C_{30} and C_{32} 1,15 diols) once stratification resumes in October. Peak abundance of the $C_{19:1}$ *n*-alkene during shallow mixing of the water column in January–February 2014 can be tentatively linked to the seasonal distribution of cyanobacteria. The concentration, seasonal variability, and low $\delta^{13}C$ values of the C_{28} fatty acid in the SPM suggest that this biomarker is produced in the water column of Lake Chala instead of having the typically assumed vascular plant origin. The $\delta^{13}C$ signature of particulate carbon and all aquatic biomarkers become increasingly more negative (by up to 16‰) during mixing-induced episodes of high productivity, whereas enrichment would be expected during such blooms. This reversed fractionation may be attributed to chemically enhanced diffusion, which generates depleted HCO_3^- under high pH (>9) conditions, as occur in the epilimnion of Lake Chala during periods of high productivity. The influence of this process can potentially explain previously observed ^{13}C-depleted carbon signatures in the paleorecord of Lake Chala, and should be considered prior to paleorecord interpretation of organic-matter $\delta^{13}C$ values derived (partially) from aquatic organisms in high-pH, i.e. alkaline, lakes.

* Corresponding author. Utrecht University, Faculty of Geosciences, Department of Earth Sciences, Princetonlaan 8A, 3584 CD, Utrecht, The Netherlands.
E-mail address: L.G.J.vanBree@uu.nl (L.G.J. van Bree).

https://doi.org/10.1016/j.quascirev.2018.05.023

1. Introduction

Lipid biomarkers are organic molecules used as indicators for the past presence of certain organisms and consequently for the past environmental conditions in which these organisms occur. For example, long-chain fatty acids ($\geq C_{24}$) and *n*-alkanes ($\geq C_{23}$) are major components of terrestrial higher (vascular) plant leaf waxes (Eglinton and Hamilton, 1967), and are, therefore, often used as biomarkers for vascular plants (e.g., Tierney et al., 2011; Sinninghe Damsté et al., 2011). Similarly, short-chain fatty acids and *n*-alkanes ($<C_{21}$) are general phytoplankton biomarkers (e.g. Gelpi et al., 1970; Meyers, 1997; Volkman et al., 1998), mid-chain *n*-alkanes (C_{21}-C_{25}) are often used as biomarkers for aquatic macrophytes (Ficken et al., 2000), and 1,15 *n*-alkyl diols are biomarkers for Eustigmatophyte algae (Volkman et al., 1992; Versteegh et al., 1997; Rampen et al., 2014; Villanueva et al., 2014).

The stable carbon-isotopic composition ($\delta^{13}C$) of these lipid biomarkers may provide further information on their origin or environmental conditions at the time of their production, and are, therefore, increasingly used in paleoclimate reconstructions (Castañeda and Schouten, 2011; Berke et al., 2012; Leng and Henderson, 2013). For example, terrestrial plants can follow several pathways of carbon fixation (C_3, C_4 and crassulacean acid metabolism (CAM)), each resulting in a different degree of fractionation of atmospheric CO_2 (Collister et al., 1994; Hobbie and Werner, 2004). As a result, analyzing compound-specific $\delta^{13}C$ of leaf waxes preserved in a lake-sediment record can be used to reconstruct vegetation history (e.g. Sinninghe Damsté et al., 2011), whereas the hydrogen isotopic composition (δD) of these leaf waxes provides additional information on past hydroclimate (e.g. Tierney et al., 2008). The $\delta^{13}C$ signature of biomarkers specific to phytoplankton can be used to trace their inorganic carbon source and the fractionation during carbon fixation (Castañeda and Schouten, 2011).

Lake sediments are a prominent archive for long-term continental paleoclimate reconstructions (Castañeda and Schouten, 2011), and especially so in tropical regions, where long ice-core and speleothem records are scarce (Verschuren, 2003; Verschuren and Russell, 2009). Organic biomarkers stored in lake sediments reflect ambient climate conditions such as temperature and precipitation prevailing in the lake's catchment at the time of their deposition. Hence, down-core variations in the occurrence, distribution, and isotopic composition of these biomarkers are increasingly used as proxies to reconstruct paleoclimate (e.g. Huang et al., 1999; Tierney et al., 2011; Berke et al., 2012). In order to strengthen the interpretation of such proxy records it is critical to understand the origin(s) and spatiotemporal variations of lipid biomarkers in modern lakes (e.g. Castañeda and Schouten, 2011). Studies documenting the distribution of specific biomarkers in sediment-trap material over a complete annual cycle, or in suspended particulate matter (SPM) along a depth profile in a stratifying lake, have improved insight in the validity of these compounds as paleoenvironmental proxies. For example, in both tropical and temperate lakes (e.g. Buckles et al., 2013, 2014; Loomis et al., 2014) the seasonal distribution of glycerol dialkyl glycerol tetraether (GDGT) membrane lipids has revealed unexpected complexity, with important implications for GDGT-based paleothermometry. This situation calls for more detailed investigations, in which the occurrence of a large range of biomarkers is analyzed both over the complete water column and through the annual cycle, and is subsequently linked to changes in environmental conditions and the composition of the lake's living microbial community.

In this study, we determine the distribution and stable carbon-isotopic composition of lipid biomarkers present in SPM from the permanently stratified water column of Lake Chala in equatorial East Africa, over a 17-month period. This tropical lake has been well-monitored, offering an excellent setting to link biomarker dynamics to water-column processes and microbial-community composition, especially in the light of future studies using lipid biomarker proxies preserved in its sedimentary record. Unique in its extent, this study provides a first thorough assessment of the occurrence and sources of organic biomarkers in lakes.

2. Material & methods

2.1. Study site

Lake Chala (locally 'Challa', after a nearby village) is a ~90 m deep and relatively unproductive crater lake on the border of Kenya and Tanzania (3°19′ S, 37°42′ E; Fig. 1). It is situated at ~880 m above sea level, on the lower east slope of Mt. Kilimanjaro. It has a surface area of ~4.5 km^2 and features a permanently stratified (meromictic) water column. As the Inter-Tropical Convergence Zone (ITCZ) is passing over the region twice a year, Lake Chala has two rain seasons, with relatively heavy 'short' rains from October to December and 'long' rains from March to May (Nicholson, 2000; Verschuren et al., 2009). The seasonal cycle of stratification and mixing in Lake Chala's water column is mainly driven by variation in air temperature and wind speed (Buckles et al., 2014; Wolff et al., 2014), with low wind speeds during the warm rain seasons leading to stratified water-column conditions, while higher wind speeds during dry seasons cause mixing, particularly during the colder southern-hemisphere winter of June–September. Evaporation (~1700 mm yr^{-1}) is higher than local precipitation (~600 mm yr^{-1}; Payne, 1970). As the small crater catchment also provides only limited surface inflow, the lake is maintained mainly by subsurface groundwater input, probably originating from Mt. Kilimanjaro's forest belt (Hemp, 2006). Mean air temperatures are lowest in July–August (20-21 °C), and highest in January–February (25-27 °C), while water-column temperature ranges from 22 °C to 28 °C (Buckles et al., 2014, 2016). Water-column mixing extends down to 40–60 m depth during the main dry season, depending on wind speed and air temperature (Verschuren et al., 2009). The resulting convective upwelling brings nutrients to the surface, which subsequently initiates phytoplankton blooms.

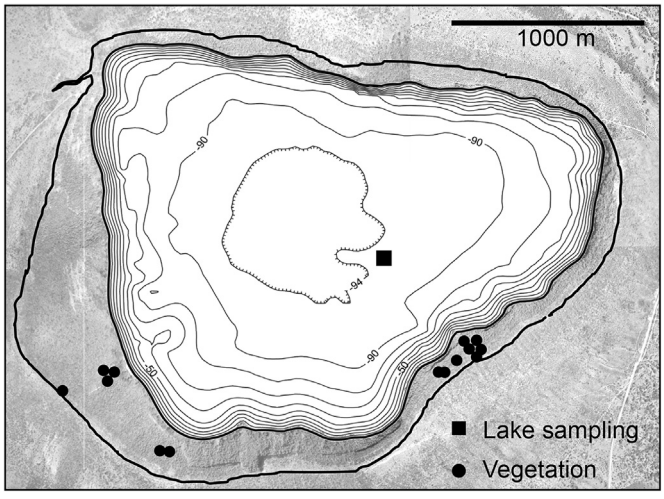

Fig. 1. Location of the measurements of physical water-column properties and sampling of SPM, phytoplankton, TIC and PC (black square) in Lake Chala; and locations of terrestrial vegetation sampling inside the crater catchment (black circles). Crater-basin map and bathymetry from Moernaut et al. (2010).

2.2. Field observations and sample collection

2.2.1. Water-column monitoring

The water column of Lake Chala was monitored at approximately four-week intervals at an offshore location 03°19.064′ S, 37°42.147′ E (Fig. 1). Physical-property profiles of the upper 50 m of the water column were collected at 1 m (0–24 m) and 2 m (24–50 m) intervals using a Hydrolab Quanta® Multiprobe which registered temperature, dissolved oxygen (DO), conductivity (K25) and pH. The pH data were corrected for drift between calibrations. Further, an air pocket in the DO sensor created unreliable DO data in the oxygenated part of the water column between 30 April and 30 June 2014.

2.2.2. Total inorganic carbon (TIC)

TIC samples were collected at the same location as the physical-property profiles, on or close to the first day of each month between September 2013 and January 2015, and from a total of 13 water depths (0, 10, 20, 25, 30, 35, 40, 45, 50, 60, 70, 80 and 90 m depth; total $n = 221$). Lake water was collected unfiltered in airtight 12 ml exetainer vials pre-poisoned with mercury chloride, and stored at room temperature. Months mentioned in the text refer to a sampling or observation date at the start of that month, or, in some cases, at the end of the previous month. The precise sampling dates are listed in Table S–2.

2.2.3. Suspended particulate matter (SPM)

SPM was collected according to the same schedule as TIC. At each depth, between 5 and 10 l of water was collected using an UWITEC water sampler. The water samples were transported in dark plastic jerrycans, filtered over pre-combusted GF/F filters (142 mm ø; Whatman) and stored frozen on the same day. The SPM samples were transported to Utrecht University on dry ice, where the filters were freeze-dried.

2.2.4. Terrestrial vegetation

Leaves from 49 plants were collected on the crater rim and near the shoreline on the Kenyan side of Lake Chala during the dry season in September 2014. The leaves were stored frozen prior to transport on dry ice, and freeze-dried at Utrecht University. Species identification was done at the National Herbarium of the Netherlands; 28 plants were identified to species level, three to genus level and five to family level, while 13 remain unidentified. Six specimens were deposited in the herbarium and can be consulted online (http://bioportal.naturalis.nl/).

2.2.5. Phytoplankton

Quantitative phytoplankton samples ($n = 85$) were taken at five depth intervals (0, 5, 10, 15 and 20 m depth) in 100 ml vials, parallel to the SPM collection but as part of an independent study of phytoplankton dynamics (C. Cocquyt, unpublished data). Immediately after collection, the lake water was fixed with an alkaline Lugol's solution prior to adding formalin.

2.3. Sample preparation and instrumental analyses

2.3.1. Bulk carbon properties

Each filter ($n = 221$) was subsampled for particulate carbon (PC) content and carbon-isotopic composition ($\delta^{13}C_{PC}$), by punching out small circles (5 mm ø). Plant samples were visually checked to remove possible contaminants such as insects and subsequently freeze-dried. A subsample of each plant was powdered for bulk organic carbon (OC) content and $\delta^{13}C$ analysis. Bulk OC (PC in case of SPM) and $\delta^{13}C$ of SPM and plants was measured using an elemental analyzer (Fisons Instruments NA1500), coupled online to an IRMS (Thermo Delta$^+$). Samples were not acidified prior to analysis, therefore representing a mixture of organic and inorganic PC in the SPM. Reproducibility of PC content was typically <0.03 μg L^{-1} ($n = 12$) for SPM, and 0.5% for OC in vegetation ($n = 7$). Reproducibility of $\delta^{13}C$ measurements was usually better than 0.1‰ based on in-house standards (nicotinamide and graphite quartzite), and <0.4‰ for PC duplicates ($n = 20$) for SPM, and 0.1‰ for vegetation ($n = 7$).

2.3.2. Total inorganic carbon

TIC concentrations in lake water were measured on a Shimadzu TOC-5050A carbon analyzer. Concentrations were calibrated using an in-house seawater standard (precision <0.3 mg L^{-1}). Replication of samples was better than 1.2 mg L^{-1} ($n = 8$). For $\delta^{13}C$ analysis of TIC, H_3PO_4 was added to vials, and vials were flushed with helium. The subsequent addition of lake water created CO_2 gas that was measured for $\delta^{13}C$ using a gas bench coupled online to an IRMS (Thermo Delta V advantage). The $\delta^{13}C$ values are reported against VPDB, using Li_2CO_3 (IAEA) and Na_2CO_3 (in-house) as standards.

2.3.3. Biomarkers

SPM filters from 0, 10, 25, 50 and 80 m depth ($n = 85$) were extracted using a modified Bligh-Dyer method (*cf.* Buckles et al., 2013). The extract was acid-hydrolyzed using 1.5N hydrochloric acid (HCl) in methanol (MeOH; 2 h reflux at 70 °C) with a known carbon isotopic composition (determined offline), and then separated into apolar, fatty-acid and polar fractions, using an activated Al_2O_3 column with hexane/dichloromethane (DCM) (9:1, v/v), DCM, and DCM/MeOH (1:1, v/v) as eluents, respectively. An aliquot of the apolar fractions was passed over an Ag^+-impregnated silicagel column with hexane and ethyl acetate (EtOAc) as eluents, respectively, to separate the saturated and unsaturated hydrocarbons.

A subset of 14 plants was selected for fatty acid analysis based on their $\delta^{13}C_{bulk}$ values (which revealed the plant's biosynthetic pathway) and habitat. Between 0.1 and 1.6 g dry weight of the leaves of each plant species was cut into small pieces, extracted ultrasonically with DCM/MeOH (2:1, v/v), and dried under a stream of N_2. An aliquot of total lipid extract was acid-hydrolyzed and separated following the same approach as for the SPM.

The apolar, fatty acid and polar fractions of SPM, as well as the fatty acid fractions of the plant samples were analyzed with a known amount of standard (pristane or 5α-cholestane) added for quantification on a gas chromatograph (GC) coupled to a flame ionization detector (GC-FID; Hewlett Packard 6890 series). All fatty acids were measured as their methyl-ester derivatives. The samples (in hexane or EtOAc as solvent) were injected on-column at 70 °C, with helium as carrier gas with a flow rate of 2 ml min^{-1}. The oven was programmed to 130 °C at 20 °C min^{-1}, and then at 4 °C min^{-1} to 320 °C at which it was held isothermal for 10 min. Selected samples were analyzed on a GC - mass spectrometer (GC-MS; Finnigan Trace GC Ultra, DSQ MS) for compound identification, with similar column properties and temperature program as the GC analysis. The mass spectral identification of biomarkers was based on comparison with a NIST library and interpretation of mass fragmentation patterns. Double-bond positions were determined by forming the adduct with dimethyl-disulfide (DMDS) and subsequent mass spectral interpretation of the products formed (Francis, 1981). Based on the GC analyses, *n*-alkane average chain length (ACL), carbon preference index (CPI) and P_{aq} were calculated as:

$$CPI = 0.5*[(\Sigma C_{25\text{-}33\text{-}odd}/\Sigma C_{26\text{-}34\text{-}even}) + (\Sigma C_{25\text{-}33\text{-}odd}/\Sigma C_{24\text{-}32\text{-}even})];$$

$$ACL = \Sigma(C_n * n)/\Sigma C_n,$$

where C_n is the abundance of each *n*-alkane with *n* carbon atoms (23–35);

$$P_{aq} = (C_{23}+C_{25})/(C_{23}+C_{25}+C_{29}+C_{31})$$

Selected fractions for compound-specific $\delta^{13}C$ measurement were injected on a GC combustion isotope-ratio-monitoring mass spectrometer (GC-C-irMS), Thermo Scientific Trace 1310 GC coupled to a Delta V mass spectrometer via an Isolink II and Conflo IV. The gas chromatograph was equipped with a PTV injector in on-column mode (on-column liner, glass, S + H Analytic, Germany) connected to a fused silica capillary column (l = 25 m; O.D. 0.32 mm) coated with CP Sil-5 (film thickness = 0.12 μm) with helium as carrier gas at a constant flow of 2 ml min^{-1}, and a similar temperature program as GC analysis, except for an additional 10 min hold at 320 °C for the plant samples. GC-C-irMS performance was checked daily by injecting an in-house GC standard combined with two fully deuterated *n*-alkanes (C_{18} and C_{24}) with known isotopic composition (IAEA). The reported values are based on at least duplicate analyses, with results averaged to obtain a mean value and standard deviation. Reproducibility is typically better than 0.7‰. $\delta^{13}C$ values are reported against the VPDB standard, with those of fatty acid methyl esters corrected for the carbon atom added during methylation. Due to co-elution with other compounds, such as non-specified triterpenoids, two of the 14 selected plant extracts were not suitable for $\delta^{13}C_{FAME}$ analysis.

2.3.4. Phytoplankton abundance

The major groups of pelagic phytoplankton (chlorophytes, diatoms, dinophytes, euglenophytes, chrysophytes, cryptophytes and cyanobacteria) were identified and counted with an inverted Olympus CKX41 microscope equipped with an Olympus UC30 digital camera, following the Utermöhl method (Utermöhl, 1931, 1958) using sedimentation chambers of 10 ml. At least 500 solitary phytoplankton cells (≥3 μm) or colonies were counted per sample, as well as the number of cells per colony. The total biovolume of each taxon present was calculated based on mean cell dimensions of the phytoplankton species, and expressed in $\mu m^3\ L^{-1}$. Euglenophytes and dinophytes are excluded from total phytoplankton biovolume due to their heterotrophic and assumed heterotrophic nature, respectively, in Lake Chala. The biovolume values were averaged across multiple sampled depths to eliminate missing values, both over the 0–10 m interval as conservative measure of the standing biomass of actively photosynthesizing phytoplankton (being proportional to primary productivity), and over the 0–20 m interval for optimal correlation with the taxon-specific biomarker concentrations. At times during the year when the latter interval extends below thermocline depth (Fig. 2), some of the phytoplankton encountered at 15 and 20 m depth must represent recently dead or dying cells in the process of sinking.

3. Results & discussion

3.1. Physical and chemical properties of the water column

3.1.1. Mixing and stratification

Variations in physical water-column properties over the period September 2013 to January 2015 (Fig. 2) mostly reflect the seasonal cycle of mixing and stratification. Changes in stratification are revealed by the temperature profiling (Fig. 2A), with high surface temperatures during stratification and lower surface temperatures particularly during the periods of deep mixing. Dissolved oxygen (DO) concentrations are influenced by oxygen diffusion from the atmosphere, temperature-driven convection, primary productivity, and oxygen consumption by the remineralization of organic matter. This interaction results in the DO profiles (Fig. 2B) being characterized by i) a shallow oxycline (between 15 and 30 m depth) during water-column stratification until June 2014, ii) oxic conditions extending down to ~40 m during July to September 2014 when deep mixing coincided with peak primary productivity, and iii) subsequent shallowing of the oxycline from October 2014 onwards due to the onset of stratification and enhanced remineralization after the algal-bloom period has ended. The difference in conductivity between epilimnion and hypolimnion over the studied interval ranges between 15 and 43 μS/cm (Fig. 2C), being small during periods of deep mixing, and larger during stratification. The epilimnion has a high pH year-round (8.3–9.0). The pH decreases from the epilimnion (pH > 8) to deeper anoxic waters in the hypolimnion (pH < 8), due to remineralization of sinking organic matter. High pH values extend down to 38 m depth during deep mixing in August–September 2014 (Fig. 2D). The seasonal trends in the water-column properties of Lake Chala observed in this study are comparable to those in previous studies (Wolff et al., 2011, 2014), but the exact timing and extent of deep mixing varies between years.

Based on these profile data, three different states of the Lake Chala water column can be recognized during the studied time interval: stratification (S), shallow mixing (SM) and deep mixing (DM). Consistent with its status as a permanently stratified (meromictic) lake, there is no evidence for complete water-column mixing during our study period. Our observations from September 2013 represent the end of a period of deeper mixing (DM), followed by stratified conditions (S) between October 2013 and May 2014. This period is shortly interrupted by a period of shallow mixing (~15 m; SM) during January–February 2014. The water column then experiences deeper mixing between June and September 2014 (DM), stratification from October 2014 to December 2014 (S), and a period of shallow mixing (SM) starting in January 2015.

3.1.2. Vertical distribution and seasonal variability in TIC and PC

The concentration of (dissolved) inorganic carbon in lakes is determined by atmospheric CO_2 exchange, primary productivity, remineralization of terrestrial and aquatic organic matter, and carbon input from runoff and groundwater inflow (Bade et al., 2004). TIC in the water column of Lake Chala consists of dissolved inorganic carbon (DIC) and suspended calcium carbonate ($CaCO_3$). TIC concentrations range from 32 mg C L^{-1} in the surface water to 56 mg C L^{-1} at depth (Fig. 3A). In a meromictic lake this increase with depth is expected, since respiration products accumulate at depth. The relatively high DIC levels in Lake Chala are primarily due to evaporation strongly exceeding precipitation, but may also originate partly from calcite-bearing tuffaceous breccia within its catchment, and make it a hard-water lake where HCO_3^- is the main anionic component (Wolff et al., 2014). The depth gradient in TIC concentration is minimal during early stratification (November 2013 to January 2014; October 2014), and TIC concentrations are low throughout the whole water column from the end of deep mixing until the end of 2014 (Fig. 3A). Within a lake the balance of production and respiration is a prime factor governing $\delta^{13}C_{TIC}$ (Striegl et al., 2001; Bade et al., 2004). The $\delta^{13}C$ of TIC is relatively high (values are less negative) in the epilimnion due to primary production preferentially removing ^{12}C, while relatively low (more negative) values occur in the hypolimnion down to 60 m (except in the early months of stratification October–December 2014), which is interpreted to reflect the remineralization of this ^{13}C-depleted organic matter as it sinks through the water column. The $\delta^{13}C$ of this respired carbon had an average value of −16.6‰, as indicated by the y-intercept of a linear trendline of $\delta^{13}C_{TIC}$ versus 1/TIC

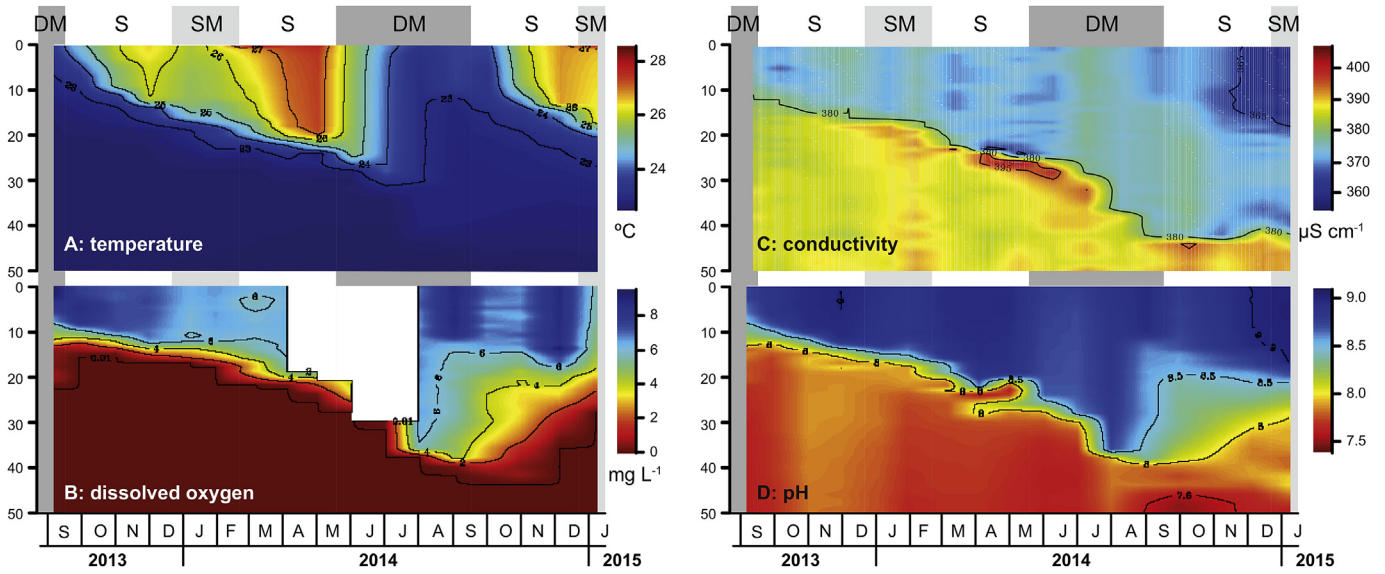

Fig. 2. Interpolated monthly profiles of temperature (A; ºC), dissolved oxygen (B; mg L^{-1}), conductivity (C; K25 in µS cm^{-1} at 25 °C) and pH (D) through the upper water column of Lake Chala (0–50 m depth), from early September 2013 until early January 2015, in relation to the periods of water-column stratification (S), shallow mixing (SM) and deep mixing (DM).

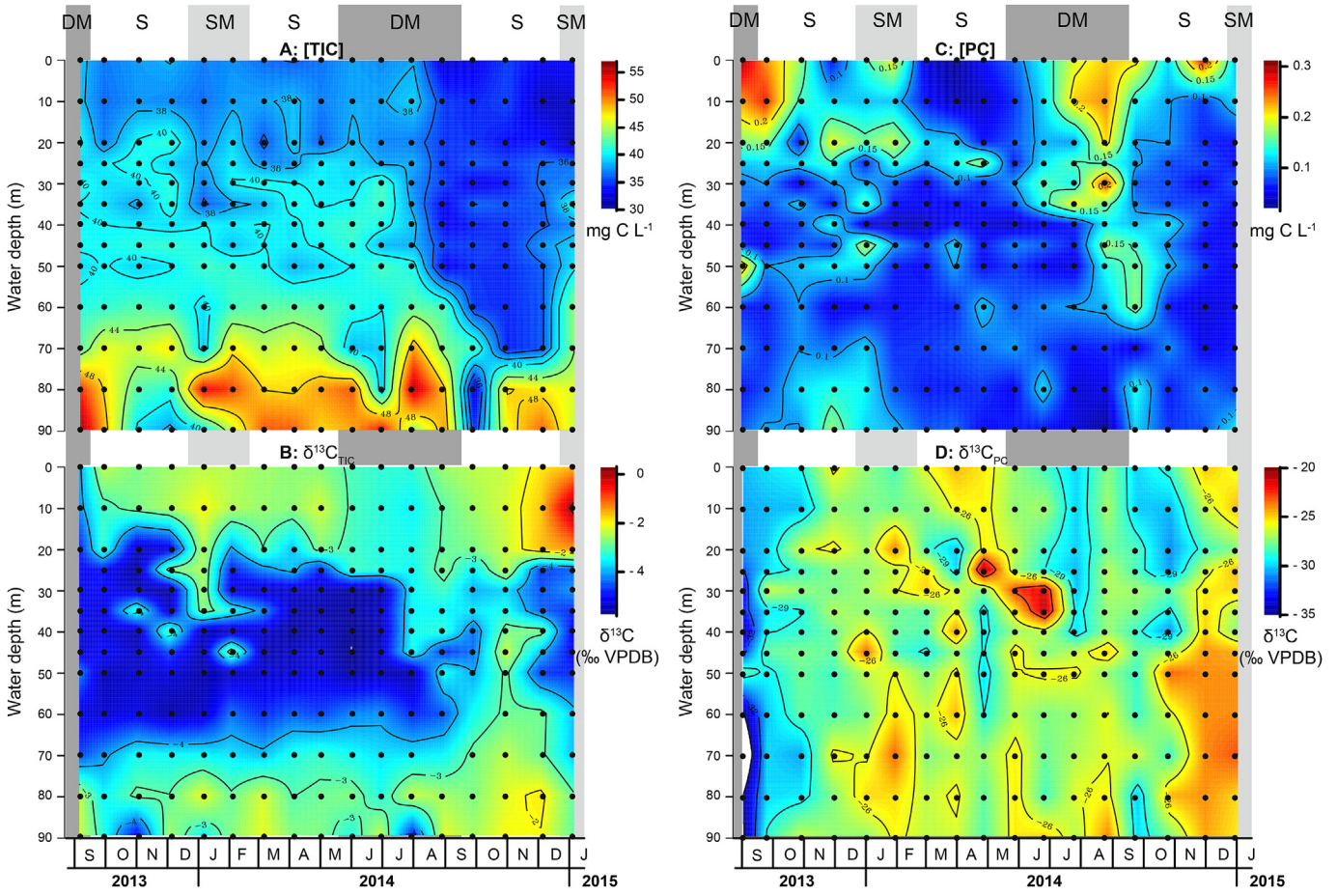

Fig. 3. Interpolated monthly profiles of concentrations (mg C L^{-1}) and $\delta^{13}C$ signature (‰ VPDB) of total inorganic carbon (TIC; A-B) and particulate carbon (PC; C-D) through the water column of Lake Chala (0–90 m depth), from early September 2013 until early January 2015, in relation to the periods of water-column stratification (S), shallow mixing (SM) and deep mixing (DM). Black dots represent the sampling depths.

concentration between 0 and 60 m depth (Keeling plot; Fig. 4). The deepest part (60–90 m) of the water column has again less negative $\delta^{13}C_{TIC}$ values, especially when TIC concentrations are also high (Fig. 3A–B). These atypically high deep-water $\delta^{13}C_{TIC}$ values can be produced by three different processes: i) subsurface inflow of water with high DIC concentration and higher $\delta^{13}C$ values; ii) methanogenesis in the bottom water or surficial sediments; and iii) $CaCO_3$ dissolution (*cf.* 'mode C' lakes; Myrbo and Shapley, 2006). In Lake Chala, all three mechanisms may be involved. Firstly, substantial subsurface inflow is needed to balance the lake's water budget (Payne, 1970), but the chemical composition of this water and depth of inflow remain unconstrained. Secondly, biomarkers for methanogenesis have been found both in the surficial sediments (Sinninghe Damsté et al., 2012) and in the anoxic deep water column (Buckles et al., 2013). And thirdly, calcite and aragonite oversaturation due to seasonal phytoplankton blooms combined with continuous strong lake-surface evaporation causes seasonally variable precipitation of $CaCO_3$ (Wolff et al., 2014). Partial dissolution of this $CaCO_3$ in the under-saturated upper hypolimnion could then enrich $\delta^{13}C_{TIC}$ in the deepest water column, while the increased TIC concentrations reflect the local accumulation of $CaCO_3$ due to its reduced sinking speed in the denser bottom water. However, the continuous pH decline with depth (Wolff et al., 2014) and presence of intact calcite crystals in the sediment record (Wolff et al., 2011) suggest that the third process may be relatively unimportant in Lake Chala.

PC concentrations range from 0.02 to 0.30 mg C L^{-1}, and generally decrease with depth (Fig. 3C), suggesting that most algae have disintegrated by the time they have sunk below 30–40 m. During mixing of the lake and until after the onset of stratification, PC concentrations are higher due to high primary productivity and greater amounts of sinking organic matter (September–October 2013; July–October 2014), while during times of prolonged stratification, PC concentrations are very low (December 2013; March–May 2014). The $\delta^{13}C_{PC}$ values range from −37.9‰ to −20.4‰ and show greater variation through time than with depth (Fig. 3D), arguing for relatively rapid sinking of organic matter. Despite substantial scatter (Fig. 3D), the lowest (most negative) $\delta^{13}C_{PC}$ values generally occur during mixing and at the onset of stratification. Overall, seasonal variation in $\delta^{13}C_{PC}$ is greater than that in $\delta^{13}C_{TIC}$, indicating that $\delta^{13}C_{PC}$ is strongly influenced by primary productivity, remineralization and mixing processes, while $\delta^{13}C_{TIC}$ is less dynamic because the TIC pool is much larger than that of PC.

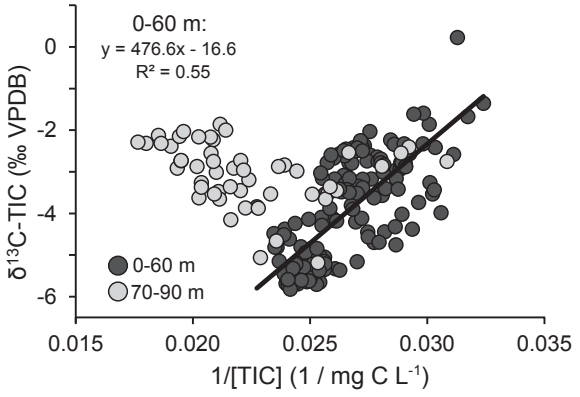

Fig. 4. Keeling plot showing the relationship between TIC $\delta^{13}C$ values (‰ VPDB) and 1/TIC concentrations (1/mg C L^{-1}), with y-intercept determined by linear regression of data from the 0–60 m depth range (black circles), and data from the 70–90 m depth range plotted for comparison (white circles).

3.2. Seasonal occurrence and possible sources of lipid biomarkers

A variety of lipid biomarkers were identified in the SPM of Lake Chala, including C_{17}-C_{35} *n*-alkanes; $C_{19:1}$ *n*-alkene; $C_{23:1}$, $C_{25:1}$ and $C_{27:1}$ *n*-alk-1-enes; phytadienes; saturated fatty acids ranging from C_{14} to C_{32} (excluding C_{19}); mono-unsaturated fatty acids (MUFAs) of C_{16}, C_{18}, C_{20}, C_{22} and C_{24}; poly-unsaturated fatty acids (PUFAs) of C_{16}, C_{18}, C_{20} and C_{22}; branched fatty acids *ai*C_{15} and *i*C_{15} to *i*C_{19}; loliolide and isololiolide; and the C_{30} and C_{32} 1,15 diols. Their respective concentrations are listed in Tables S-2 to S-4, and their $\delta^{13}C$ values in Table S–5. To permit comparison to other variables, SPM biomarker concentrations were integrated over the upper 25 m of the water column (average of 0, 10 and 25 m), unless stated otherwise. Here we discuss a selection of the most common biomarkers (Fig. 5) that show strong seasonal changes and/or have clear potential as paleo-environmental proxy.

3.2.1. Biomarkers of eukaryote phytoplanktonts

Most groups of primary producers contain chlorophyll, a source of phytol (e.g. Rontani and Volkman, 2003). Acid hydrolysis of lipid extracts containing phytol can produce phytadienes (Grossi et al., 1996). Although phytadienes are thus secondary products, they are a direct reflection of phytol (and thereby chlorophyll) concentration in the SPM. Therefore, we here use the sum of all phytadienes (Fig. 5A) as a general indicator of changes in the total biomass of aquatic primary producers in Lake Chala. The $\delta^{13}C$ value of these phytadienes in our data set ranges between −34.4 and −30.3‰, i.e. relatively enriched in ^{13}C compared to other aquatic biomarkers, due to their isoprenoidal structure (*cf.* Schouten et al., 1998). The concentration of phytadienes is highest in September 2013 and between June and November 2014 (i.e. during and immediately after deep mixing), and also elevated between December 2013 and February 2014, at the start of shallow mixing. The phytadiene concentrations have a seasonal pattern similar to that of the total biomass of autotrophic phytoplankton (as measured by their total biovolume; Fig. 6A–B) and PC concentrations (Fig. 6C) in the upper 0–10 m. This also confirms that our PC values mainly represent POC, although PIC, in the form of precipitating calcite crystals, likely contributed to the modest PC maxima during the warm shallow-mixing periods of January–February 2014 and January 2015 (*cf.* Wolff et al., 2014). Additionally, seasonal variation in Secchi-disk depth (Fig. 6D), an indicator of light penetration, corresponds with the PC concentrations. The seasonal pattern in all these variables is conform the expectation that primary productivity is enhanced during and just after periods of deep water-column mixing, due to upwelling of nutrients from the hypolimnion (Buckles et al., 2014).

The concentration of long-chain *n*-alk-1-enes ($C_{23:1}$, $C_{25:1}$ and $C_{27:1}$) increases during the main period of deep mixing (Fig. 5D), with relatively high concentrations extending down to 80 m water depth in October 2014 (Table S–2). The highest concentrations of these long-chain *n*-alk-1-enes were found between July and November 2014 in the epilimnion, up to 1.3 μg L^{-1} at the surface in August 2014. The distribution of these long-chain *n*-alkenes is similar in all samples, translated in strong correlation of their individual concentrations ($C_{23:1}$-$C_{25:1}$ $R^2 = 0.96$; $C_{25:1}$-$C_{27:1}$ $R^2 = 0.96$; $C_{23:1}$-$C_{27:1}$ $R^2 = 0.90$; $n = 72$); in general, the concentration of $C_{27:1}$ is higher than that of $C_{25:1}$ and $C_{23:1}$. Also the $\delta^{13}C$ values of the *n*-alk-1-enes are similar, and range between −41.0 and −36.6‰ ($C_{23:1}$), −40.9 and −35.3‰ ($C_{25:1}$), −41.8 and −35.8‰ ($C_{27:1}$) (Table S–5), suggesting a common source. Their seasonal pattern (Figs. 5C–7A) matches well with that of total biovolume estimates for Chlorophyta (green algae; Fig. 7B). Specifically, *Tetraedron minimum*, which is often the dominant chlorophyte in Lake Chala, is similarly distributed with time as the *n*-alk-1-enes (Fig. 7C *versus*

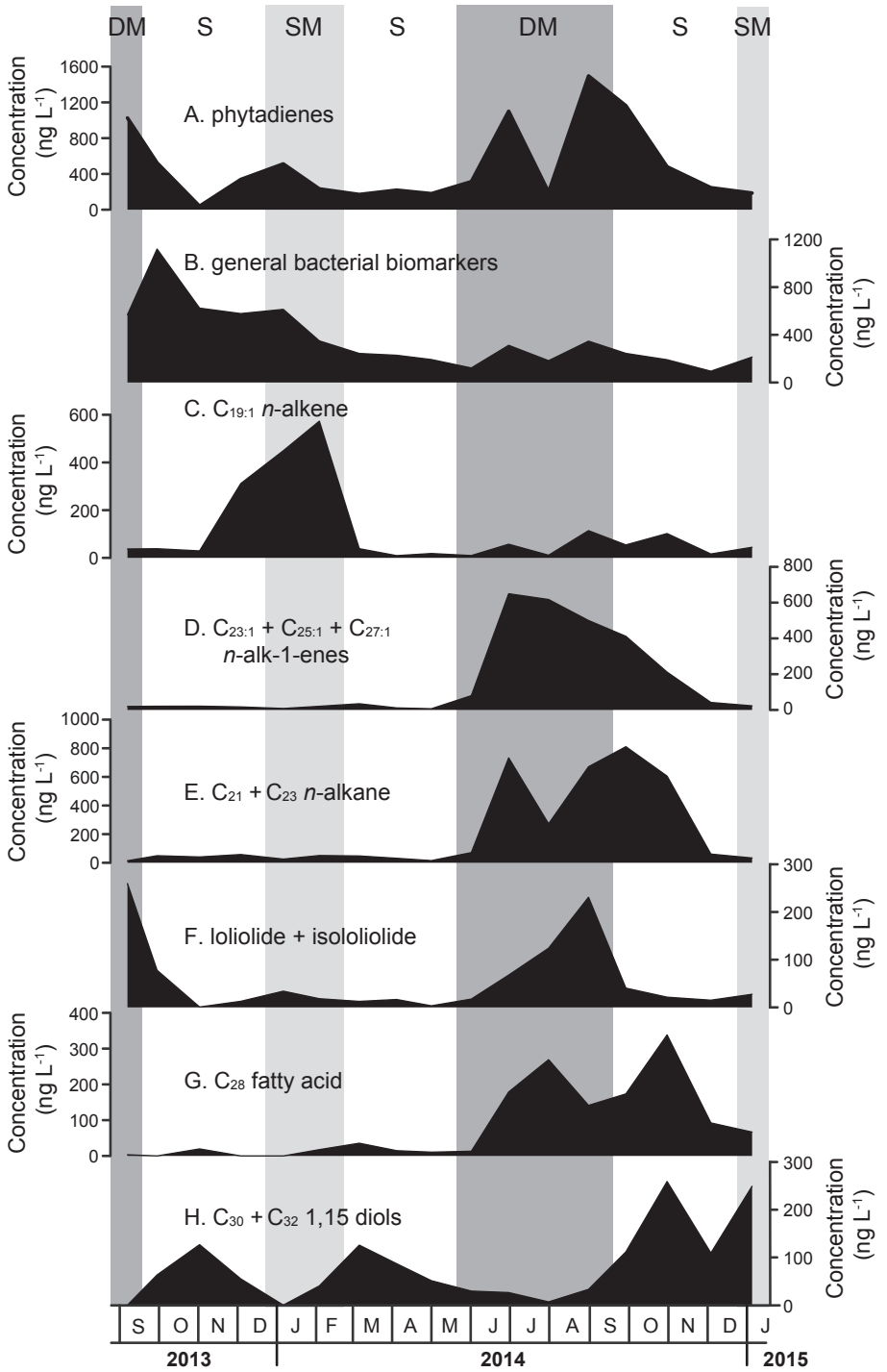

Fig. 5. Seasonal variation in the concentration (in ng L^{-1}) of selected biomarkers in SPM from the upper 25 m (average of 0, 10 and 25 m depth) of Lake Chala, in relation to the periods of water-column stratification (S), shallow mixing (SM) and deep mixing (DM). A: Summed phytadienes. B: Summed general bacterial biomarkers *ai*-C_{15}, *i*-C_{15}, *i*-C_{16}, *i*-C_{17} and *i*-C_{19} fatty acids. C: $C_{19:1}$ *n*-alkene. D: Summed $C_{23:1}$, $C_{25:1}$ and $C_{27:1}$ *n*-alk-1-enes. E: Summed C_{21} and C_{23} mid-chain *n*-alkanes. F: Summed loliolide and isololiolide. G: C_{28} fatty acid. H: Summed C_{30} and C_{32} 1,15 *n*-alkyl diols.

7A) and seems, therefore, the most likely source organism of those compounds in Lake Chala, even though *n*-alk-1-enes had previously not been detected in cultures of *T. minimum* (Gelpi et al., 1970). Based on similarities between the *n*-alk-1-enes and phytoplankton abundances in settling particles and SPM collected in 2007, van Bree et al. (2014) proposed that the green algae *Cosmarium* spp. might be a possible source for these compounds in Lake Chala. Our present study indicates that *T. minimum* is more likely the dominant source organism, given that the total biovolume of *Cosmarium* spp. is an order of magnitude lower than that of *T. minimum,* and the timing of its bloom (Fig. 7D) more distinct from that of the long-chain *n*-alk-1-enes. Nevertheless, it remains possible that the long-chain *n*-alk-1-enes in Lake Chala are produced by several chlorophyte taxa.

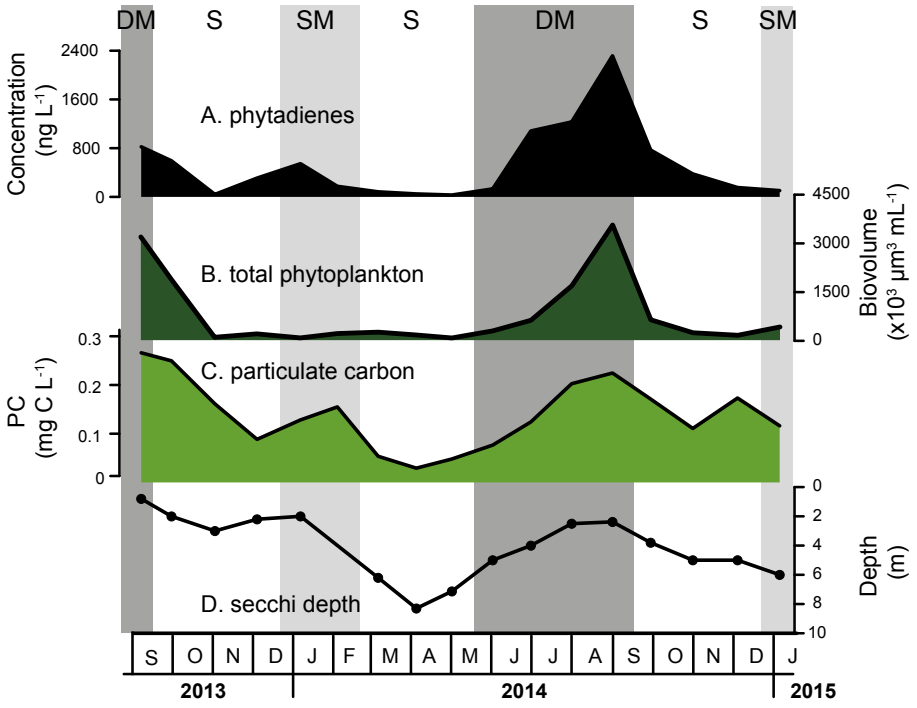

Fig. 6. Seasonal variation in summed phytadiene concentration in SPM (A) and three measures of total primary production (B–D), all in relation to the periods of water-column stratification (S), shallow mixing (SM) and deep mixing (DM). A-C represent average values over the 0–10 m depth interval. A: Summed phytadienes (in ng L^{-1}). B: Phytoplankton biomass, expressed as biovolume (x10^3 µm^3 L^{-1}). C: Concentration of particulate carbon (mg C L^{-1}). D: Secchi depth (m).

The seasonal distribution of the mid-chain length *n*-alkanes C_{21} and C_{23} are highly similar to each other (Fig. 7E–F; Table S–2), and their summed distribution (Fig. 5E) is comparable to those of the *n*-alk-1-enes. The $\delta^{13}C$ values of C_{21} and C_{23} *n*-alkanes range between −43.8 and −36.2‰ (Table S–5) and are nearly identical at specific times and depths ($R^2 = 0.97$, $n = 5$). The relative abundance of these mid-chain *n*-alkanes in lake sediment records (expressed as P_{aq}; Ficken et al., 2000) is often linked to the past presence of submerged or emergent macrophytes, although these compounds also occur in algae (e.g. the green alga *Tetraedron* sp.; Gelpi et al., 1970). In our data, P_{aq} is always above 0.4, excluding two samples that lack C_{23} and C_{25} *n*-alkanes altogether. This would normally be interpreted as a macrophyte-dominated *n*-alkane pool. However, a significant source of submerged macrophytes is unlikely in Lake Chala (Sinninghe Damsté et al., 2011; van Bree et al., 2016) due to its steep rocky shores (Moernaut et al., 2010), and also our isotope data indicate that an algal source is much more likely. Most probably, the C_{21} and C_{23} *n*-alkanes in Lake Chala SPM are biomarkers for chlorophyte algae, considering their seasonal timing, $\delta^{13}C$ values, and similarity between the total chlorophyte and *n*-alk-1-ene abundances.

Bacillariophyta (diatoms) are important primary producers in Lake Chala, as reflected in the high fractional abundance of diatom valves in the sediment record (Wolff et al., 2011; Barker et al., 2011, 2013). The biomarkers loliolide and isololiolide are degradation products of the diatom pigment fucoxanthin (Klok et al., 1984; Repeta, 1989). Although some Haptophyta and Dinophyta species have also been reported as possible sources of this pigment (Klok et al., 1984; Jeffrey and Vesk, 1997), loliolide and isololiolide are generally held indicative of diatom input, especially when haptophyte algae are absent (Castañeda et al., 2009; Castañeda and Schouten, 2011), such as in Lake Chala. The combined loliolide and isololiolide concentration (Fig. 5F) peaks in September of both 2013 and 2014, reaching up to 450 ng L^{-1} (September 2014, 25 m depth). The seasonal pattern of loliolide and isololiolide is indeed similar to that of total diatom biovolume (Fig. 8A–B). The most important diatom species in Lake Chala are *Nitzschia fabiennejansseniana* (Cocquyt and Ryken, 2017, Fig. 8C), *Afrocymbella barkeri* (Cocquyt and Ryken, 2016, Fig. 8D) and, to a lesser extent, *Ulnaria/Fragilaria* spp. (Fig. 8E; C. Cocquyt unpublished data). Although there is large variation in the relative abundance of these diatoms between the deep-mixing periods of 2013 and 2014, loliolide and isololiolide do not seem to track a specific species, but appear to reflect total diatom production in Lake Chala, in line with the ubiquitous occurrence of fucoxanthin in diatoms.

C_{30} and C_{32} 1,15 diols commonly occur in lake sediments, and are known biomarkers for Eustigmatophyta in marine and freshwater environments (Volkman et al., 1992, 1999; Rampen et al., 2014; Villanueva et al., 2014). In Lake Chala they occur in high abundance between October and December 2013, February to June 2014, and October 2014 to January 2015 (Fig. 5H), i.e. consistently during the periods with a stratified water column. Relatively little is known about eustigmatophyte ecology in lakes, as these cells are often overlooked in phytoplankton counts due to their small size and non-diagnostic appearance. Their absence in our phytoplankton dataset indicates that the cells of Lake Chala species are either smaller than 3 µm, or not preserved intact despite fixation with an alkaline Lugol's solution prior to adding formalin. The C_{30} and C_{32} 1,15 diols in Lake Chala were previously studied in sediment-trap samples as part of material settling through the water column between August 2009 and 2010 (Villanueva et al., 2014). That study identified five eustigmatophyte groups based on the detection of 18S rRNA genes, and showed that these algae are important producers of long-chain diols in Lake Chala. The documented seasonal changes in diol abundance are also in line with our findings. This indicates that eustigmatophytes thrive, more than other algal groups, under stratified conditions, and hence that sedimentary C_{30} and C_{32} 1,15 diol records have the potential to serve as proxy for past stratified conditions in Lake Chala.

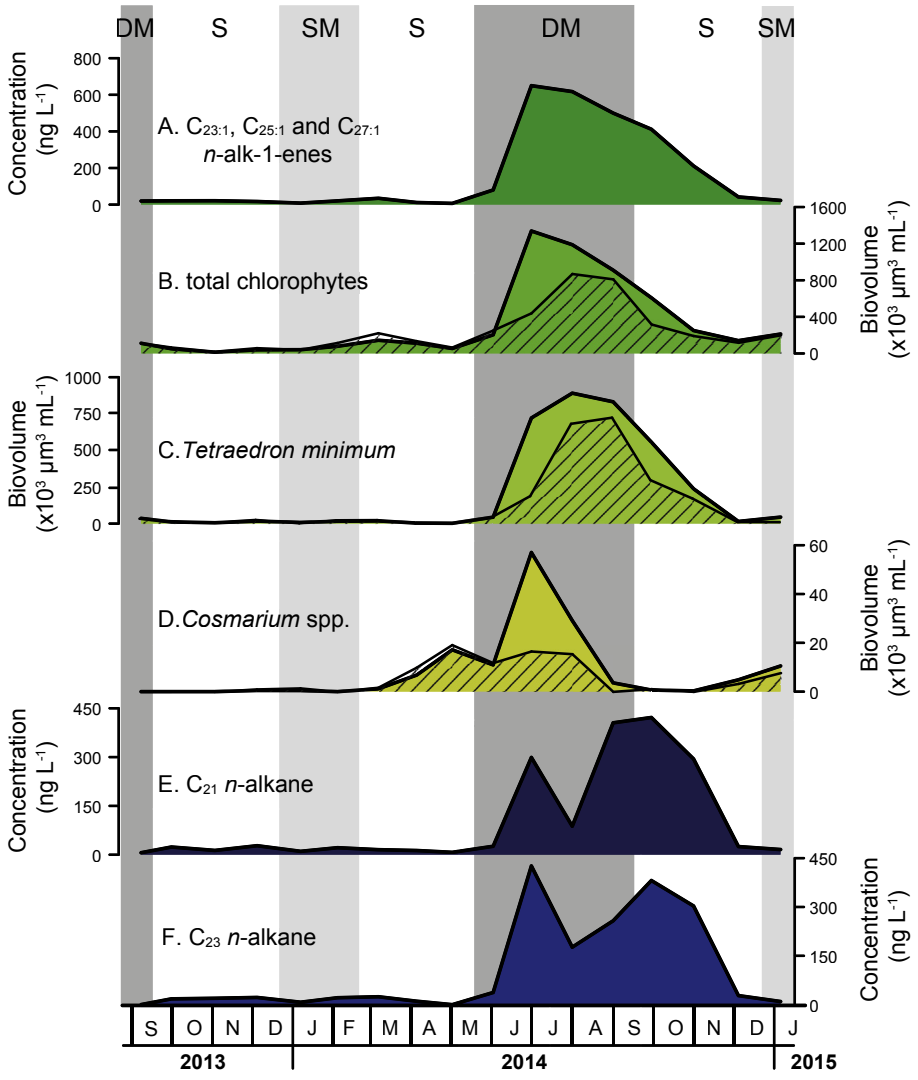

Fig. 7. Seasonal variation in summed $C_{23:1}$, $C_{25:1}$ and $C_{27:1}$ *n*-alk-1-ene (A), C_{21} *n*-alkane (E) and C_{23} *n*-alkane (F) concentrations in Lake Chala SPM (all in ng L^{-1}) compared with seasonal patterns in total (B) and selected (C–D) chlorophyte algae, in relation to the periods of water-column stratification (S), shallow mixing (SM) and deep mixing (DM). B: Total chlorophytes. C: *Tetraedron minimum*. D: *Cosmarium* spp., all total biomass expressed as biovolume (x10^3 µm^3 L^{-1}). A, E and F represent average values over 0–25 m depth, whereas B-D show average values integrated over 0–10 m depth (open diagonal lines) and 0–20 m depth (filled surfaces); see text of section 2.3 for argumentation.

3.2.2. Biomarkers of (cyano-)bacteria

In our data from the upper water column of Lake Chala, general biomarkers for bacteria such as short-chain *iso* and *anteiso* fatty acids (FA) reach peak values during or immediately after periods of high primary production, and decrease in abundance during periods of stratification (Figs. 5B and 9A). The magnitude of the peak that developed after the main mixing season of 2014 is much less than the one that developed after the mixing season of 2013, notwithstanding the comparable total phytoplankton abundance (Fig. 6B). Although some bacterial biomarkers such as *iso*C_{16} and *iso*C_{19} FAs were mostly found in the anoxic deeper water column, and concentrations of *iso*C_{15} and *anteiso*C_{15} FAs decrease noticeably below the epilimnion, in general bacterial biomarkers are found throughout the water column (Table S–3).

One bacterial biomarker with a distinct seasonal pattern is the $C_{19:1}$ *n*-alkene, which develops a prominent peak between December 2013 and March 2014, i.e. mostly during the period of shallow mixing (Fig. 9B). Concentrations of $C_{19:1}$ *n*-alkene reach 0.7 µg L^{-1} in the upper 10 m of the water column in January–February 2014, and decrease in deeper water. Its compound-specific $\delta^{13}C$ values range from −43.2 to −35.6‰. Short-chain *n*-alkenes (<C_{22}) are generally assumed to be derived from cyanobacteria or microalgae (e.g. Gelpi et al., 1968, 1970; Volkman et al., 1998). Although the $C_{19:1}$ *n*-alkene is not commonly used in biomarker studies, it can be synthesized by cyanobacteria, and has been reported in cultures of the marine cyanobacteria *Coccochloris elabens* and *Agmenelium quadruplicatum* (Winters et al., 1969), *Synechococcus* sp. (marine strain PCC7002; ~38% of total hydrocarbons; Coates et al., 2014; Mendez-Perez et al., 2014) and *Leptolyngbya* sp. (strain PAC 10-3; ~98% of total hydrocarbons; Coates et al., 2014). The peak $C_{19:1}$ *n*-alkene concentration during shallow mixing does indeed suggest a cyanobacterial source rather than other phytoplankton groups, which all display other seasonal patterns (Figs. 6B, 7B and 8B). Although the seasonal trend in total biovolume of all identified cyanobacteria (Fig. 9C) does not directly correspond to that of $C_{19:1}$ *n*-alkene (Fig. 9B), the seasonal pattern of *Planktolyngbya* and related taxa, one of the dominant groups of cyanobacteria in Lake Chala, is similar in that it also displays a prominent peak during the shallow mixing season of 2014 (Fig. 9D). *Planktolyngbya* is closely related to *Leptolyngbya* species, which is

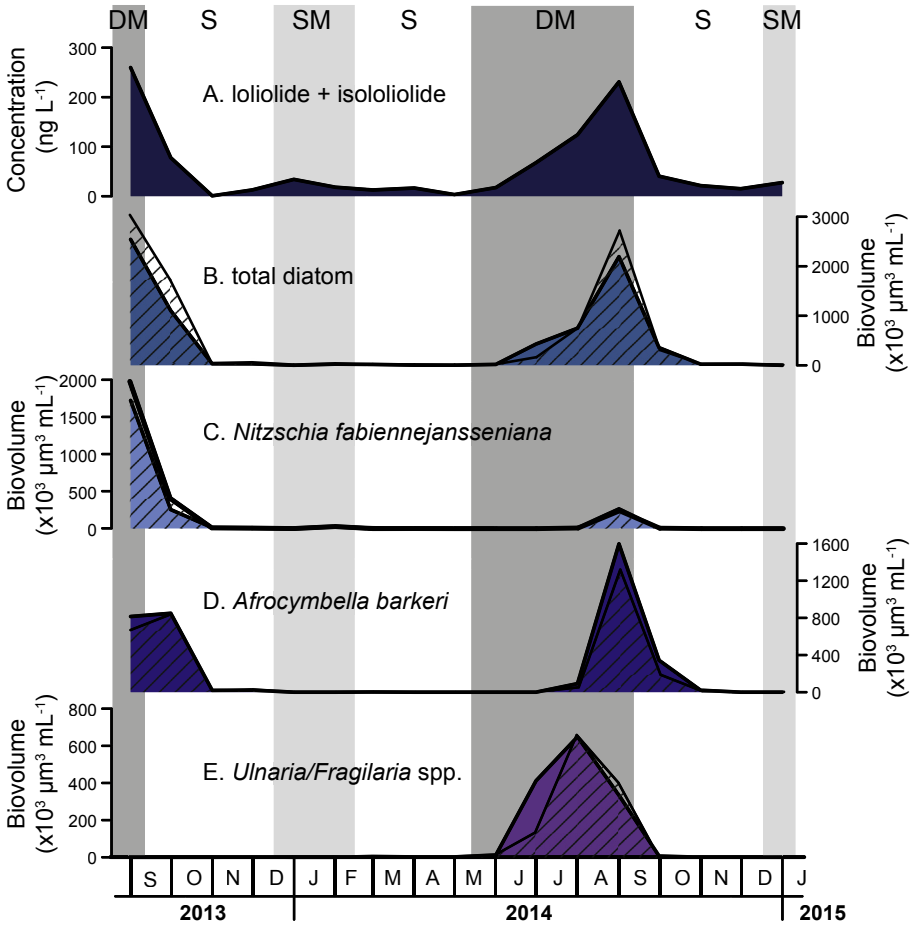

Fig. 8. Seasonal variation in summed loliolide-isololiolide concentration in Lake Chala SPM (A; in ng L^{-1}) compared with seasonal patterns in total (B) and selected (C–E) diatom algae, in relation to the periods of water-column stratification (S), shallow mixing (SM) and deep mixing (DM). B: Total diatoms. C: *Nitzschia fabiennejansseniana*. D: *Afrocymbella barkeri*. E: *Ulnaria/Fragilaria* spp., all expressed as biovolume (x10^3 µm^3 L^{-1}). A represents average values over 0–25 m depth, whereas B-E show average values over 0–10 m depth (open diagonal lines) and 0–20 m depth (filled surfaces); see text of section 2.3 for argumentation.

known to produce $C_{19:1}$ *n*-alkenes (Coates et al., 2014). *Synechococcus* sp. (>3 µm) seems a less likely source of the $C_{19:1}$ *n*-alkenes here (Fig. 9E). Further, the seasonal trend in $C_{19:1}$ *n*-alkene concentration closely matches that of the cyanobacterial photoactive pigment myxoxanthophyll (pers. comm. H. Tanttu, Ghent University). Considering this similar timing and the relatively high concentration of $C_{19:1}$ *n*-alkene in Lake Chala, and its occurrence in cyanobacterial cultures (Winters et al., 1969; Coates et al., 2014; Mendez-Perez et al., 2014), it seems most likely that the $C_{19:1}$ *n*-alkene in Lake Chala has a cyanobacterial origin, and may potentially be used as biomarker specific to cyanobacteria.

3.2.3. Biomarkers of terrestrial vegetation

Long-chain *n*-alkanes derived from vascular plants are present in low concentrations (max. 92 ng L^{-1}, July 2014 at the surface; Table S–2), often too low for accurate quantification. Vascular plants typically have a strong odd-over-even *n*-alkane distribution. Therefore, high carbon preference index (CPI) values are indicative of a terrestrial plant origin, while CPI values ~1 indicate a bacterial or algal *n*-alkane source (Gelpi et al., 1970; Cranwell et al., 1987). The CPI of the *n*-alkanes in Lake Chala SPM varies between 0.2 and 4.6 (1.6 on average), indicating limited contribution of terrestrial-plant *n*-alkanes. ACL varies between 23.3 and 28.6 (26.3 on average). The mean $\delta^{13}C$ values of long-chain *n*-alkanes are -29.5 ± 0.8‰ (C_{29}, $n = 4$), -30.9 ± 1.7‰ (C_{31}, $n = 4$) and -31.2 ± 1.6‰ (C_{33}, $n = 3$). Long-chain FAs are present mainly during the deep-mixing period and subsequent start of stratification. The most abundant FA is C_{22}, followed by C_{28} and C_{24}. Their $\delta^{13}C$ values range from −41.5 to −27.3‰ (C_{20} FA), −39.6 to −26.8‰ (C_{24} FA), −41.9 to −26.7‰ (C_{26} FA), and −46.3 to −34.3‰ (C_{28} FA). Due to co-elution, $\delta^{13}C$ of the C_{22} FA could only be determined in five samples, and ranges from −39.3 to −31.5‰. Compared to the long-chain *n*-alkanes, the $\delta^{13}C$ of long-chain FAs have a larger range and reach much greater negative values. Since their concentration maxima also have a different timing over the studied period, the long-chain FAs are, therefore, likely not exclusively terrestrial (see section 3.3).

The (near-) absence of biomarkers for terrestrial vegetation in the SPM of Lake Chala during the sampled period is striking, as these biomarkers are clearly present in the sediments (e.g. Sinninghe Damsté et al., 2011; van Bree et al., 2016). This suggests that SPM, even when sampled throughout a full year, must still be considered to represent a 'snapshot' in time, mainly reflecting processes within the water column, rather than a reflection of all preserved settling particles that contribute to the sedimentary record.

3.2.4. Inter-annual variability

In this unproductive lake with permanently anoxic bottom waters and strong seasonal stratification of the upper water

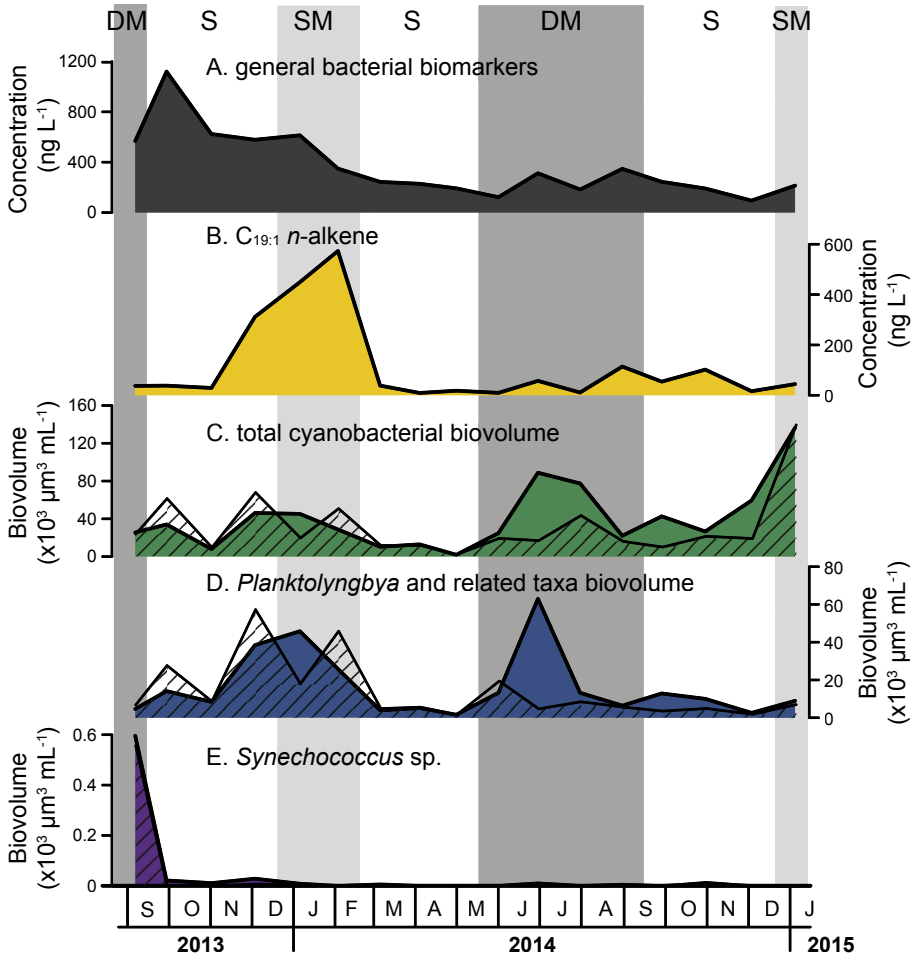

Fig. 9. Seasonal variation in the summed concentrations of general bacterial biomarkers *ai*-C_{15}, *i*-C_{15}, *i*-C_{16}, *i*-C_{17} and *i*-C_{19} FAs (A) and the $C_{19:1}$ *n*-alkene in Lake Chala SPM (B; both in ng L^{-1}) compared with seasonal patterns in total (C) and selected (D–E) cyanobacteria, in relation to the periods of water-column stratification (S), shallow mixing (SM) and deep mixing (DM). C: Total cyanobacteria. D: *Planktolyngbya* and related taxa. E: *Synechococcus* sp., all expressed as biovolume (x10^3 µm^3 L^{-1}). A-B represent average values over 0–25 m depth, whereas C-E show average values over 0–10 m depth (open diagonal lines) and 0–20 m depth (filled surfaces); see text of section 2.3 for argumentation.

column, primary productivity critically depends on the annual recurrence of deep mixing (to 45–60 m depth since 1999; Buckles et al., 2014) and associated upwelling of nutrients. Overall, phytoplankton biomass (as reflected in phytadiene and PC concentrations, and in total biovolume) is highest during the two periods of deep mixing covered by this study (Fig. 6). However, when looking at specific biomarkers, substantial inter-annual differences are evident between the periods September 2013 to January 2014 and September 2014 to January 2015. Diatom blooms (producing loliolide and isololiolide) recur yearly and have similar timing and abundance, while chlorophytes (C_{21} and C_{23} *n*-alkanes; $C_{23:1}$, $C_{25:1}$ and $C_{27:1}$ *n*-alkenes) bloomed only in 2014. Eustigmatophytes (C_{30} and C_{32} 1,15 diols) were common during all periods with a stratified water column in both years. Physical water-column conditions, such as the duration and depth of seasonal water-column mixing, are key controls on phytoplankton abundance and species succession. In Lake Chala, inter-annual variation in the duration and depth of mixing, and hence the inter-annual variation in biomarker succession, is partly due to local climate variability linked to the El Niño-Southern Oscillation (ENSO), where El Niño years are wetter, and La Niña years drier (Nicholson, 2000; Nicholson and Selato, 2000; Wolff et al., 2014). In particular, the phytoplankton blooming season in Lake Chala is extended during La Niña years, while El Niño years have a shorter blooming season and more abrupt onset of water column stratification (Wolff et al., 2011). During the time interval covered by this study, El Niño conditions (although relatively weak) from October 2014 onwards (http://www.cpc.ncep.noaa.gov/products/analysis_monitoring/ensostuff/ensoyears.shtml) are reflected in a more abrupt onset of temperature stratification in 2014 than in 2013 (Fig. 2A), which may in turn have influenced the seasonal succession of phytoplankton and the biomarkers derived from them. The time period covered by this study is, however, too short to draw firm conclusions about the proximate and ultimate causes of inter-annual variation in the biomarker distributions.

3.3. Aquatic source of C_{28} FA in Lake Chala

The C_{28} FA is the most abundant long-chain fatty acid in SPM between C_{26} and C_{32} (76% of C_{max}; $n = 64$), with concentrations up to 390 ng L^{-1} in November 2014 (Fig. 10A). The strong seasonal pattern of C_{28} FA in the water column of Lake Chala suggests that this compound has an aquatic source. However, long-chain FAs in sediment records are usually assumed to be derived from terrestrial vascular plants (e.g. Eglinton and Eglinton, 2008; Tierney et al., 2010; Castañeda and Schouten, 2011; Freeman and Pancost, 2014; Hemingway et al., 2016), because they are a major component of leaf waxes (Eglinton and Hamilton, 1967; Kolattukudy, 1976). Yet

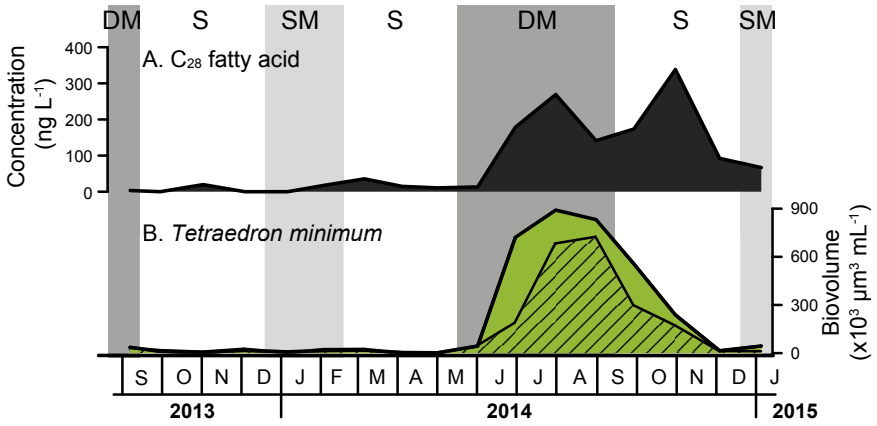

Fig. 10. Seasonal variation in C_{28} fatty acid concentration in Lake Chala SPM (A; in ng L^{-1}) compared with seasonal patterns in the chlorophyte algae *Tetraedron minimum* (B; in biovolume in x10^3 µm^3 L^{-1}), in relation to the periods of stratification (S), shallow mixing (SM) and deep mixing (DM). A represents average values over 0–25 m depth, whereas B-C show average values over 0–10 m depth (open diagonal lines) and 0–20 m depth (filled surfaces); see text of section 2.3 for argumentation.

long-chain FAs are also known to occur in algae and (cyano-)bacteria (e.g. Volkman et al., 1980, 1998), and there have been several, although infrequent, warnings about possible aquatic production interfering with the terrestrial plant signal (e.g. Feakins et al., 2007; Kusch et al., 2010; Holland et al., 2013).

In order to check whether long-chain FAs in Lake Chala are indeed derived from terrestrial plants, we started by comparing the distribution and $\delta^{13}C$ values of long-chain FA homologues in the SPM with that in vegetation from the crater, i.e. the most likely source of vascular plant wax lipids in Lake Chala (Sinninghe Damsté et al., 2011). The distribution of FAs in plant leaves ($n = 14$) varies widely between plant species (Table S–1) and ranges from C_{14} to C_{37} with an average chain length ($ACL_{FAME20-37}$) of 26.4 ± 1.4. Further, C_{max} varies between 24 and 32, and the FAs have a strong even-over-odd carbon number predominance. The $\delta^{13}C$ values of leaf waxes from C_3 plants vary between −41.3 and −32.4‰ (with a weighted average $\delta^{13}C$ value between −37.8 and −34.7‰ among species), while the C_4 grasses have FA $\delta^{13}C$ values between −20.9 and −24.5‰ (weighted average of −21.6‰ and −22.7‰; Table S–1). Vegetation-derived FA distributions ($n = 14$) are clearly different from those in SPM (averaged; $n = 71$) (Fig. 11), as C_{28} and C_{30} FAs co-dominate in vegetation, whereas C_{30} FAs are hardly detected in SPM and C_{28} is by far the most dominant long-chain FA. Further, the $\delta^{13}C$ of FA homologues in SPM (Fig. 12A) and terrestrial plants (Fig. 12B) also indicate that the latter C_{28} FA does not reach the level of ^{13}C depletion recorded in SPM. Considering that vegetation around Lake Chala is a mixture of C_3, C_4 and CAM plants

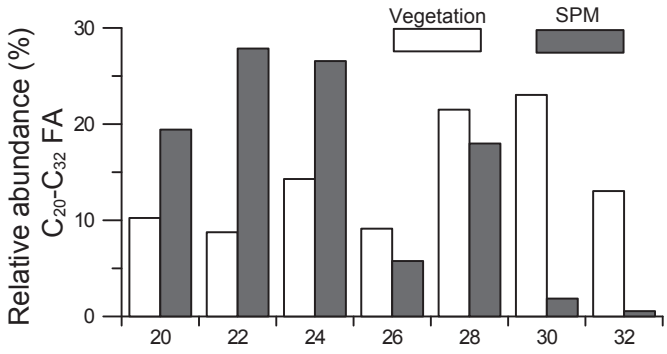

Fig. 11. Contrasting average distribution of fatty acids with carbon number C_{20} to C_{32} in SPM from Lake Chala (dark grey; $n = 79$) and in terrestrial vegetation surrounding the lake (white; $n = 14$).

(Sinninghe Damsté et al., 2011), an average plant-derived C_{28} FA signature in the sediment would be relatively enriched, due to the C_{28} FAs contributed by C_4 and CAM plants. Moreover, C_{28} FAs in SPM show a ~12‰ shift in $\delta^{13}C$ between July and November 2014, that cannot be explained other than by aquatic production (see Section 3.4). Although some contribution of C_{28} FAs from terrestrial plants cannot be excluded, the distinct FA-homologue distribution patterns and $\delta^{13}C$ values clearly indicate that there is extensive aquatic C_{28} FA production in the water column of Lake Chala.

A few microalgae, including (marine) diatoms and chlorophytes, are known to produce some long-chain FAs between C_{20} and C_{30}, usually in small amounts (Volkman et al., 1980, 1989; 1998; Rezanka and Podojil, 1986). Specifically, C_{28} FA was found in the fresh-water chlorophyte *Scenedesmus communis* (recently transferred to the genus *Desmodesmus*) and a batch culture of *Tetraedron minimum* (Schouten et al., 1998), and was part of the insoluble biopolymer algaenan of both species (Blokker et al., 1998). *Scenedesmus* can be excluded as possible significant source organisms in Lake Chala, considering its overall rarity (three occurrences of small colonies entailing <0.5% of total counted cells of these samples) and a seasonal distribution entirely different from that of the C_{28} FA. *T. minimum* is a more likely source, because it is a common species and reaches greatest abundance during the mixing season of July–September 2014, coincident with one of two prominent peaks in the seasonal pattern of C_{28} FA (Fig. 10). However, we hesitate to assign the origin of C_{28} FA to *Tetraedron*, because C_{28} FA concentration peaks during both the mixing and subsequent stratification periods, and it also occurs (albeit in lesser quantities) during the two other monitored stratification periods when *Tetraedron* is almost absent from the phytoplankton counts.

3.4. Seasonal trends in particulate-carbon and biomarker $\delta^{13}C$

An overview of seasonal trends in the $\delta^{13}C$ values of selected biomarkers (Fig. 13) shows that all lipid biomarkers that are probably derived from algae blooming during (or immediately following) the June-to-September 2014 period of deep mixing (long-chain *n*-alk-1-enes, C_{21} and C_{23} *n*-alkanes, C_{26} and C_{28} FAs) become increasingly depleted in ^{13}C (up to 14.7‰ lighter), reaching values as low as −41.8‰ ($C_{27:1}$ *n*-alkene) and −46.3‰ (C_{28} FA) by the end of October 2014. This depletion is also reflected in the moderately decreasing values of $\delta^{13}C_{PC}$ during this deep-mixing period (up to 4.5‰, averaged over the depth interval 0–10 m; Fig. 3D), but is not seen in $\delta^{13}C_{TIC}$, which shows a slight enrichment

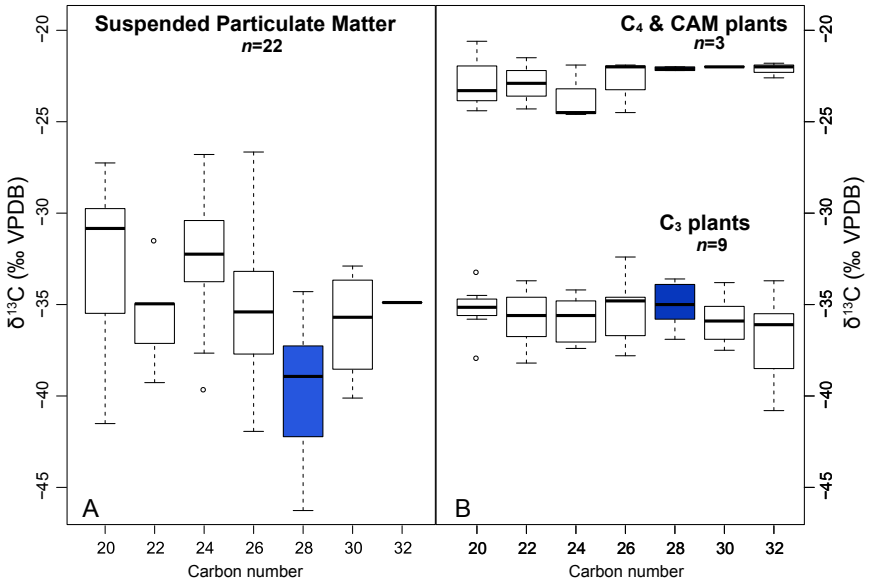

Fig. 12. Boxplots of the $\delta^{13}C$ values (‰ VPDB) of C_{20} to C_{32} fatty acids (median, first and third quartiles, whiskers depicting minimum and maximum values, and outliers as open symbols) in SPM from Lake Chala (A; $n = 22$) and in C_3 plants (B; $n = 9$) and C_4+CAM plants (C; $n = 2 + 1$) from surrounding terrestrial vegetation. The C_{28} fatty acid is accentuated in blue. (For interpretation of the references to colour in this figure legend, the reader is referred to the Web version of this article.)

of ~1‰ within the epilimnion during this time period (Fig. 3B). Whereas the latter trend is expected, the depletion trend in biomarker and particulate-carbon $\delta^{13}C$ is not, because growing phytoplankton preferentially takes up ^{12}C, thereby enriching the epilimnetic pool of DIC. During a pronounced blooming period, the phytoplankton also incorporate this relatively enriched DIC and become more and more enriched in ^{13}C themselves. However, instead of this expected enrichment we see a systematic depletion (ranging from ~4.4‰ to ~14.7‰) in bulk $\delta^{13}C_{PC}$ and various lipid biomarkers derived from algal organic matter. A temporal switch from CO_2 to HCO_3^--uptake by these primary producers cannot explain the large difference in fractionation, because HCO_3^- is enriched in ^{13}C relative to CO_2 by ~8‰ (Mook et al., 1974) and hence HCO_3^- utilization would lead to ^{13}C enrichment, and not depletion, of the resulting organic matter. The $\delta^{13}C$ depletion trend during times of higher productivity is also reflected in the $C_{19:1}$ *n*-alkene, the suspected cyanobacterial biomarker which is produced primarily during the shallow mixing period of January–February 2014 (Fig. 13A), indicating that this atypical ^{13}C depletion is not a time-specific or species-specific phenomenon, but strongly suggests a universal phenomenon in the water column of Lake Chala during episodes of enhanced primary production. In order to explain this large depletion in PC and aquatic-biomarker $\delta^{13}C$, we need a source of depleted DIC that is not reflected in the $\delta^{13}C_{TIC}$.

Several possible water-column sources of ^{13}C-depleted DIC exist, such as upwelling of ^{13}C-depleted hypolimnetic water, or enhanced input of ^{13}C-depleted CH_4 and its oxidation to CO_2. It is possible that part of the depleted DIC pool in the photic zone of Lake Chala originates from respired DIC ($\delta^{13}C$ of ~−16.6‰, Fig. 4) that is brought upwards from the hypolimnion during deep mixing, but it is unlikely that all depleted DIC results from upwelling as the difference in $\delta^{13}C_{TIC}$ between surface and the most depleted water around 50 m depth is not very large (between −1.3 and −5.4‰; Fig. 3B). Moreover, the long duration of enhanced depletion is inconsistent with mixing from deeper water as the primary mechanism, as the largest depletion occurs after the onset of stratification in October 2014, when any upwelling of depleted carbon must have stopped.

Release of CH_4 depleted in ^{13}C from the lower water column and bottom sediments, and its subsequent oxidation to CO_2, might also contribute to ^{12}C-rich DIC. Although it would be expected that methanotroph biomarkers have low $\delta^{13}C$ values, it is surprising that all phytoplankton-derived biomarkers become increasingly depleted in ^{13}C. Unless there is an extremely tight coupling between methanotrophy and primary production in Lake Chala, it is unlikely that methanotrophy plays a substantial role in the ^{13}C depletion of its DIC. Thus, the depletion of $\delta^{13}C$ in PC and aquatic biomarkers cannot be explained with carbon sources from 'the deep', i.e. upwelling of respired or CH_4-derived carbon.

The main alternative source of ^{13}C-depleted carbon is the atmosphere, since CO_2 dissolves into under-saturated lake waters. Typically, dissolved CO_2 reacts with H_2O to form HCO_3^-. However, at high pH conditions it increasingly reacts with OH^- (Herczeg and Fairbanks, 1987), which leads to chemically enhanced diffusion. This process can mitigate carbon limitation in aquatic biological processes (Portielje and Lijkema, 1995), and can have significant influence on the air-water CO_2 flux and carbon residence time in lakes (Wanninkhof and Knox, 1996). The process of chemically enhanced diffusion is well documented in gas-transfer models and laboratory measurements, and has also been reported in a few natural lake settings (Bade and Cole, 2006, and references therein; Portielje and Lijkema, 1995; Bontes et al., 2006; Lammers et al., 2017). This process may take place in Lake Chala, as it has high epilimnetic pH values (8.3–9.0 during our period of observation) particularly during episodes of high primary production (Fig. 2D). Not only is the flux of CO_2 into the water column enhanced, the reaction of CO_2 with OH^- results in strong carbon-isotopic fractionation: +8‰ in the common reaction of CO_2 with H_2O to produce HCO_3^-, but −15‰ in the reaction of CO_2 with OH^- (Mook et al., 1974; Herczeg and Fairbanks, 1987; Bade and Cole, 2006). There are two periods when this process of chemically enhanced fractionation seems evident in the PC and biomarker $\delta^{13}C$ values in Lake Chala: during shallow mixing in January–February 2014, and during/after deep mixing between August and November 2014. The biomarkers are on average ~12.8‰ (long-chain fatty acids), ~7.4‰ (C_{21} and C_{23} *n*-alkanes), and ~4.9‰ (long-chain *n*-alkenes) more

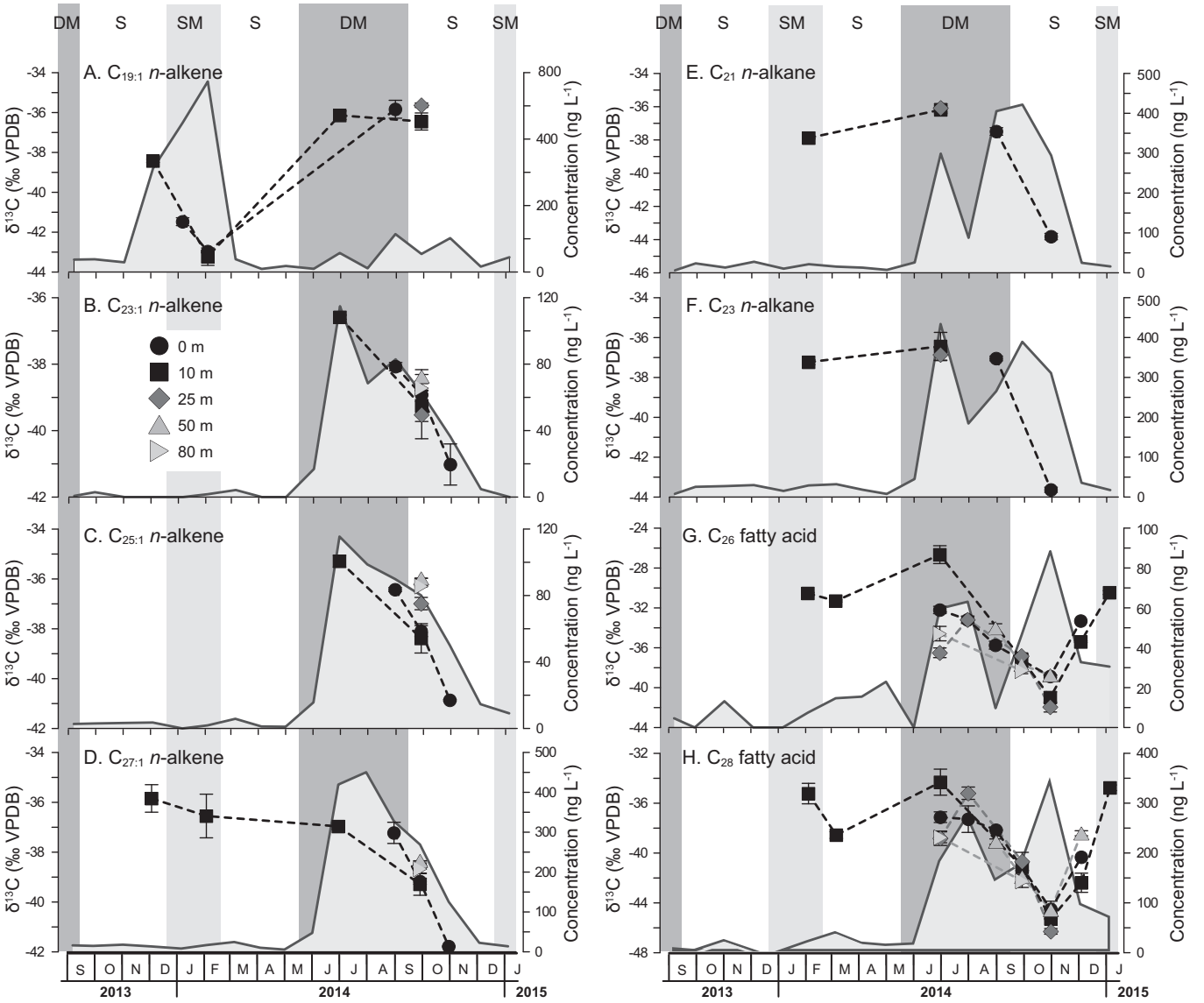

Fig. 13. Variation in the $\delta^{13}C$ values (‰ VPDB) of selected biomarkers (A–H) in the SPM of Lake Chala over the period September 2013 to January 2015, from the surface (0 m) and 10, 25, 50 and 80 m depth (symbol legend in panel B), in relation to periods of stratification (S), shallow mixing (SM) and deep mixing (DM). The concentration of each biomarker (ng L^{-1}; averaged over 0–25 m depth) is depicted in the background. Note that $\delta^{13}C$ values of the $C_{19:1}$ *n*-alkene decrease coincident with high production during the SM period (A), whereas $\delta^{13}C$ values of all other biomarkers decrease coincident with high production during the DM period (B–H). B: $C_{23:1}$ *n*-alk-1-enes. C: $C_{25:1}$ *n*-alk-1-enes. D: $C_{27:1}$ *n*-alk-1-enes. E: C_{21} *n*-alkane. F: C_{23} *n*-alkane. G: C_{26} fatty acid. H: C_{28} fatty acid.

depleted in November 2014 than at the start of the mixing induced phytoplankton bloom. The variation in $\delta^{13}C_{PC}$ within the epilimnion is relatively small (~4.5‰) compared to that in the biomarkers, which is unexpected. At this time, we speculate that this might be due to strong CO_2 depletion and high pH halos immediately around the microorganisms generating strongly ^{13}C-depleted HCO_3^- locally, which is not reflected in overall $\delta^{13}C_{TIC}$ values but does substantially influence the $\delta^{13}C$ values of the algal biomarkers.

3.5. Implications for paleoenvironmental reconstruction

The high seasonal variability in the modern lake system of Lake Chala implies that seasonal variability may on the one hand complicate interpretation of the paleoenvironmental record, but on the other hand provide new insights on past seasonality. Given the atypical carbon-isotope fractionation process occurring in modern-day Lake Chala, we need to be careful when interpreting sedimentary carbon-isotope signatures as reflecting the enrichment or depletion of various carbon sources in the past. Whether chemically enhanced fractionation could be an important confounding factor will likely depend on the extent to which the naturally high pH of Lake Chala (and many other East African lakes, fresh or saline) is increased further by seasonally high photosynthetic activity. Not only the compound-specific carbon-isotopic signature of aquatic lipid biomarkers, but also of organic matter encapsulated in diatom frustules (Barker et al., 2013), or of bulk algal matter contributing to the $\delta^{13}C$ value of sedimentary TOC (Blaauw et al., 2011) are likely to be influenced by this process. The magnitude of ^{13}C depletion which we recorded in the SPM of Lake Chala during the peak phytoplankton bloom may also hint at the importance of chemically enhanced fractionation in the past, i.e. whether in any particular period the boundary conditions of epilimnetic water pH > 8 were met. At least throughout the studied 25-kyr sediment record of Lake Chala, aquatic-biomarker $\delta^{13}C$

values have been characteristically low. The $\delta^{13}C$ values of $C_{25:1}$ *n*-alk-1-ene and $C_{27:1}$ *n*-alk-1-ene vary, respectively, from −42.2 to −37.3‰, and from −44.0 to −38.8‰ (van Bree et al., 2014), and those of the C_{23} *n*-alkane reach values as low as −48‰ (Sinninghe Damsté et al., 2011). The organic matter within diatom frustules is also relatively depleted in ^{13}C, with values between −36.4 and −27.3‰ (Barker et al., 2013).

Secondly, paleohydrological and paleovegetation reconstructions based on the hydrogen-isotope and carbon-isotope signatures of the C_{28} fatty acid, respectively, are made on the premise that this compound is solely terrestrial, as are the leaf-wax alkanes. An aquatic origin, or mixed terrestrial/aquatic origin, of C_{28} FA therefore poses a problem for paleoclimate studies. When the $\delta^{13}C$ signature of long-chain FAs is used as proxy for vegetation type, input of the relatively ^{13}C-depleted aquatic C_{28} FA may substantially overestimate the fraction of C_3 vegetation present. Because compound-specific δD measurement requires relatively high biomarker concentrations, and C_{28} FA is often the most abundant FA homologue in East African lakes, it has frequently been used to reconstruct past δD fluctuations in precipitation, not only in Lake Chala (Tierney et al., 2011) but also in Lake Tanganyika (Tierney et al., 2008), Lake Victoria (Berke et al., 2012), Lake Turkana (Morrissey, 2014) and Lake Tana (Costa et al., 2014). Moreover, this dominance of the C_{28} FA is not exclusively an East African phenomenon but also occurs in, for example, Lake El'gygytgyn in Siberia (Holland et al., 2013). A predominantly aquatic production of the C_{28} FA indicates that its δD signature records photic-zone lake-water composition rather than meteoric water modified by the evapotranspiration processes in soils and plants. While long-term trends in δD may still be comparable, the amplitude of the paleorecord will be smoothed as precipitation δD is spatially and temporally integrated in aquatic δD sources (Sachse et al., 2012); and the potential temporal resolution of the paleorecord will be limited by (and be proportional to) lake residence time. Consequently, regional/global syntheses of paleohydrological studies should be careful when interpreting absolute δD changes based on the C_{28} FA, and when integrating those δD records with those based on "real" plant waxes. When using *n*-alkanes as plant-wax biomarkers for δD reconstruction is not feasible, we recommend supplementary $\delta^{13}C$ measurements on the FA used, to check if their values are consistent with a vascular plant origin. Meanwhile, more research is also needed to identify the specific aquatic sources of C_{28} FA.

4. Conclusion

This study used monthly collections of SPM from throughout the water column of Lake Chala, supplemented by $\delta^{13}C$ analyses of the TIC and PC, to trace seasonal variability in the concentration, distribution and carbon-isotopic signature of lipid biomarkers in relation to seasonal succession in the lake's algal and microbial communities. After deep mixing started upwelling nutrients from the hypolimnion in June 2014, there is a succession in the phytoplankton from chlorophyte to diatom and then eustigmatophyte dominance, each producing characteristic biomarker compounds: $C_{23:1}/C_{25:1}/C_{27:1}$ *n*-alk-1-enes and C_{21}/C_{23} *n*-alkanes (chlorophytes), loliolide/isololiolide (diatoms), C_{30}/C_{32} 1,15 diols (eustigmatophytes). The $C_{19:1}$ *n*-alkene can be tentatively linked to cyanobacteria. Based on concentration, seasonal variability, and the $\delta^{13}C$ values of C_{28} FA in SPM, we argue that this biomarker is produced in the water column of Lake Chala, instead of having a terrestrial vascular plant origin as is usually assumed. While future research will have to clarify the actual source of this C_{28} FA in lakes, this aquatic production should be kept in mind when interpreting the $\delta^{13}C$ and δD signatures of long-chain FAs extracted from sediment records. Finally we observed strong ^{13}C depletion in various aquatic carbon pools during seasons of high primary production. This is likely the result of high pH (>9) in Lake Chala's photic zone during such bloom periods, a condition promoting chemically enhanced carbon fractionation. This process can explain the strongly depleted organic carbon in the sediment record of Lake Chala as well as other high-pH lakes, and might potentially form the basis to develop a new biomarker-based surface-water pH proxy.

Acknowledgements

We thank P. Meyers and an anonymous reviewer for their feedback on the manuscript. We thank C.M. Oluseno for conducting the monthly sampling and other field assistance in Kenya. Sample collection was carried out with permission of the Permanent Secretary of the Ministry of Education, Science and Technology of Kenya, through research permit 13/001/11C to D.V. We thank W.I.C. Rijpstra and J.W. de Leeuw (NIOZ) for discussions on analytical methods; H. Tanttu (UGent) for providing unpublished pigment data; J.F. Veldkamp (Naturalis, Leiden) for help with taxonomy of the grass species; and C. Wolff (Max Planck Institute of Chemistry, Mainz) and M. Lammers (UU) for discussions on the carbon system in lakes. We are also grateful to A. van Dijk, D. Kasjaniuk, A. van Leeuwen-Tolboom, D. van den Meent-Olieman, C. Mulder, K. Nierop (UU) and J. Ossebaar (NIOZ) for technical and analytical support. This research was supported by the NESSC Gravitation Grant (024.002.001) from the Dutch Ministry of Education, Culture and Science (OCW) to J.S.S.D.

Appendix A. Supplementary data

Supplementary data related to this article can be found at https://doi.org/10.1016/j.quascirev.2018.05.023.

References

Bade, D.L., Carpenter, S.R., Cole, J.J., Hanson, P.C., Hesslein, R.H., 2004. Controls of $\delta^{13}C$-DIC in lakes: geochemistry, lake metabolism, and morphometry. Limnol. Oceanogr. 49, 1160–1172.

Bade, D.L., Cole, J.J., 2006. Impact of chemically enhanced diffusion on dissolved inorganic carbon stable isotopes in a fertilized lake. J. Geophys. Res. 111. C01014.

Barker, P.A., Hurrell, E.R., Leng, M.J., Wolff, C., Cocquyt, C., Sloane, H.J., Verschuren, D., 2011. Seasonality in equatorial climate over the past 25 k.y. revealed by oxygen isotope records from Mount Kilimanjaro. Geology 39, 1111–1114.

Barker, P.A., Hurrell, E.R., Leng, M.J., Plessen, B., Wolff, C., Conley, D.J., Keppens, E., Milne, I., Cumming, B.F., Laird, K.R., Kendrick, C.P., 2013. Carbon cycling within an East African lake revealed by the carbon isotope composition of diatom silica: a 25-ka record from Lake Challa, Mt. Kilimanjaro. Quat. Sci. Rev. 66, 55–63.

Berke, M.A., Johnson, T.C., Werne, J.P., Schouten, S., Sinninghe Damsté, J.S., 2012. A mid-Holocene thermal maximum at the end of the African Humid Period. Earth Planet Sci. Lett. 351–352, 95–104.

Blokker, P., Schouten, S., van den Ende, H., de Leeuw, J.W., Hatcher, P.G., Sinninghe Damsté, J.S., 1998. Chemical structure of algaenans from the fresh water algae *Tetraedron minimum, Scenedesmus communis* and *Pediastrum boryanum*. Org. Geochem. 29, 1453–1468.

Bontes, B.M., Pel, R., Ibelings, B.W., Boschker, H.T.S., Middelburg, J.J., van Donk, E., 2006. The effects of biomanipulation on the biogeochemistry, carbon isotopic composition and pelagic food web relations of a shallow lake. Biogeosciences 3, 69–83.

van Bree, L.G.J., Rijpstra, W.I.C., Cocquyt, C., Al-Dhabi, N.A., Verschuren, D., Sinninghe Damsté, J.S., de Leeuw, J.W., 2014. Origin and palaeo-environmental significance of C_{25} and C_{27} *n*-alk-1-enes in a 25,000-year lake-sedimentary record from equatorial East Africa. Geochem. Cosmochim. Acta 145, 89–102.

van Bree, L.G.J., Rijpstra, W.I.C., Al-Dhabi, N.A., Verschuren, D., Sinninghe Damsté, J.S., de Leeuw, J.W., 2016. *Des*-A-lupane in an East African lake sedimentary record as a new proxy for the stable carbon isotopic composition of C_3 plants. Org. Geochem. 101, 132–139.

Blaauw, M., van Geel, B., Kristen, I., Plessen, B., Lyaruu, A., Engstrom, D.R., van der Plicht, J., Verschuren, D., 2011. High-resolution ^{14}C dating of a 25,000-year lake-sediment record from equatorial East Africa. Quat. Sci. Rev. 30, 3043–3059.

Buckles, L.K., Villanueva, L., Weijers, J.W.H., Verschuren, D., Sinninghe Damsté, J.S., 2013. Linking isoprenoidal GDGT membrane lipid distributions with gene

abundances of ammonia-oxidizing Thaumarchaeota and uncultured crenarchaeotal groups in the water column of a tropical lake (Lake Challa, East Africa). Environ. Microbiol. 15, 2445–2462.
Buckles, L.K., Weijers, J.W.H., Verschuren, D., Sinninghe Damsté, J.S., 2014. Sources of core and intact branched tetraether membrane lipids in the lacustrine environment: anatomy of Lake Challa and its catchment, equatorial East Africa. Geochem. Cosmochim. Acta 140, 106–126.
Buckles, L.K., Verschuren, D., Weijers, J.W.H., Cocquyt, C., Blaauw, M., Sinninghe Damsté, J.S., 2016. Interannual and (multi-)decadal variability in the sedimentary BIT index of Lake Challa, East Africa, over the past 2200 years: assessment of the precipitation proxy. Clim. Past 12, 1243–1262.
Castañeda, I.S., Werne, J.P., Johnson, T.C., 2009. Influence of climate change on algal community structure and primary productivity of Lake Malawi (East Africa) from the Last Glacial Maximum to present. Limnol. Oceanogr. 54, 2431–2447.
Castañeda, I.S., Schouten, S., 2011. A review of molecular organic proxies for examining modern and ancient lacustrine environments. Quat. Sci. Rev. 30, 2851–2891.
Cocquyt, C., Ryken, E., 2016. *Afrocymbella barkeri* spec. nov. (Bacillariophyta), a common phytoplankton component of Lake Challa, a deep crater lake in East Africa. Eur. J. Phycol. 51, 217–225.
Cocquyt, C., Ryken, E., 2017. Two new needle-shaped *Nitzschia* taxa from a deep East African crater lake. Diatom Res. 32, 465–475.
Collister, J.W., Rieley, G., Stern, B., Eglinton, G., Fry, B., 1994. Compound-specific $\delta^{13}C$ analyses of leaf lipids from plants with differing carbon dioxide metabolisms. Org. Geochem. 21, 619–627.
Coates, R.C., Podell, S., Korobeynikov, A., Lapidus, A., Pevzner, P., Sherman, D.H., Allen, E.E., Gerwick, L., Gerwick, W.H., 2014. Characterization of cyanobacterial hydrocarbon composition and distribution of biosynthetic pathways. PLoS One 9 e85140.
Costa, K., Russell, J., Konecky, B., Lamb, H., 2014. Isotopic reconstruction of the african humid period and Congo air boundary migration at Lake Tana, Ethiopia. Quat. Sci. Rev. 83, 58–67.
Cranwell, P.A., Eglinton, G., Robinson, N., 1987. Lipids of aquatic organisms as potential contributors to lacustrine sediments II. Org. Geochem. 11, 513–527.
Eglinton, G., Hamilton, R.J., 1967. Leaf epicuticular waxes. Science 156, 1322–1335.
Eglinton, T.I., Eglinton, G., 2008. Molecular proxies for paleoclimatology. Earth Planet Sci. Lett. 275, 1–16.
Feakins, S.J., Eglinton, T.I., deMenocal, P.B., 2007. A comparison of biomarker records of northeast African vegetation from lacustrine and marine sediments (ca. 3.40 Ma). Org. Geochem. 38, 1607–1624.
Ficken, K.J., Li, B., Swain, D.L., Eglinton, G., 2000. An *n*-alkane proxy for the sedimentary input of submerged/floating freshwater aquatic macrophytes. Org. Geochem. 31, 745–749.
Francis, G.W., 1981. Alkylthiolation for the determination of double-bond position in unsaturated fatty acid esters. Chem. Phys. Lipids 29, 369–374.
Freeman, K.H., Pancost, R.D., 2014. Biomarkers for terrestrial plants and climate. In: Falkowski, P., Freeman, K. (Eds.), Treatise on Geochemistry, vol. 12. Elsevier, Amsterdam, pp. 395–416.
Gelpi, E., Oró, J., Schneider, H.J., Bennett, E.O., 1968. Olefins of high molecular weight in two microscopic algae. Science 161, 700–702.
Gelpi, E., Schneider, H.J., Mann, J., Oró, J., 1970. Hydrocarbons of geochemical significance in microscopic algae. Phytochemistry 9, 603–612.
Grossi, V., Baas, M., Schogt, N., Klein Breteler, W.C.M., de Leeuw, J.W., Rontani, J.-F., 1996. Formation of phytadienes in the water column: myth or reality? Org. Geochem. 24, 833–839.
Hemingway, J.D., Schefuß, E., Dinga, B.J., Pryer, H., Galy, V.V., 2016. Multiple plant-wax compounds record differential sources and ecosystem structure in large river catchments. Geochem. Cosmochim. Acta 184, 20–40.
Hemp, A., 2006. Continuum or zonation? Altitudinal gradients in the forest vegetation of Mt. Kilimanjaro. Plant Ecol. 184, 27–42.
Herczeg, A.L., Fairbanks, R.G., 1987. Anomalous carbon isotope fractionation between atmospheric CO_2 and dissolved inorganic carbon induced by intense photosynthesis. Geochem. Cosmochim. Acta 51, 895–899.
Hobbie, E.A., Werner, R.A., 2004. Intramolecular, compound-specific, and bulk carbon isotope patterns in C_3 and C_4 plants: a review and synthesis. New Phytol. 161, 371–385.
Holland, A.R., Petsch, S.T., Castañeda, I.S., Wilkie, K.M., Burns, S.J., Brigham-Grette, J., 2013. A biomarker record of Lake El'gygytgyn, far east Russian Arctic: investigating sources of organic matter and carbon cycling during marine isotope stages 1-3. Clim. Past Discuss 9, 243–260.
Huang, Y., Street-Perrott, F.A., Perrott, R.A., Metzger, P., Eglinton, G., 1999. Glacial–interglacial environmental changes inferred from molecular and compound-specific $\delta^{13}C$ analyses of sediments from Sacred Lake, Mt. Kenya. Geochim. Cosmochim. Acta 63, 1383–1404.
Jeffrey, S.W., Vesk, M., 1997. Introduction to marine Phytoplankton and Their Pigment Signatures. in: Phytoplankton Pigments in Oceanography: Guidelines to Modern Methods. UNESCO, Paris, pp. 37–84.
Klok, J., Baas, M., Cox, H.C., de Leeuw, J.W., Schenck, P.A., 1984. Loliolides and dihydroactinidiolide in a recent marine sediment probably indicate a major transformation pathway of carotenoids. Tetrahedron Lett. 25, 5577–5580.
Kolattukudy, P., 1976. Chemistry and Biochemistry of Natural Waxes. Elsevier, Amsterdam, 459 pp.
Kusch, S., Rethemeyer, J., Schefuß, E., Mollenhauer, G., 2010. Controls on the age of vascular plant biomarkers in Black Sea sediments. Geochem. Cosmochim. Acta 74, 7031–7047.
Lammers, J.M., Reichart, G.J., Middelburg, J.J., 2017. Seasonal variability in phytoplankton stable carbon isotope ratios and bacterial carbon sources in a shallow Dutch lake. Limnol. Oceanogr. 62, 2773–2787.
Leng, M.J., Henderson, A.C., 2013. Recent advances in isotopes as palaeolimnological proxies. J. Paleolimnol. 49, 481–496.
Loomis, S.E., Russell, J.M., Heureux, A.M., D'Andrea, W.J., Sinninghe Damsté, J.S., 2014. Seasonal variability of branched glycerol dialkyl glycerol tetraethers (brGDGTs) in a temperate lake system. Geochem. Cosmochim. Acta 144, 173–187.
Mendez-Perez, D., Herman, N.A., Pfleger, B.F., 2014. A desaturase gene involved in the formation of 1,14-nonadecadiene in *Synechococcus* sp. Strain PCC 7002. Appl. Environ. Microbiol. 80, 6073–6079.
Meyers, P.A., 1997. Organic geochemical proxies of paleoceanographic, paleolimnologic, and paleoclimatic processes. Org. Geochem. 27, 213–250.
Moernaut, J., Verschuren, D., Charlet, F., Kristen, I., Fagot, M., De Batist, M., 2010. The seismic-stratigraphic record of lake-level fluctuations in Lake Challa: hydrological stability and change in equatorial East Africa over the last 140 kyr. Earth Planet Sci. Lett. 290, 214–223.
Mook, W.G., Bommerson, J.C., Staverman, W.H., 1974. Carbon isotope fractionation between dissolved bicarbonate and gaseous carbon dioxide. Earth Planet Sci. Lett. 22, 169–176.
Morrissey, A., 2014. Stratigraphic Framework and Quaternary Paleolimnology of the Lake Turkana Rift. Doctoral dissertation, Syracuse University, Kenya.
Myrbo, A., Shapley, M.D., 2006. Seasonal water-column dynamics of dissolved inorganic carbon stable isotopic compositions ($\delta^{13}C$ DIC) in small hardwater lakes in Minnesota and Montana. Geochem. Cosmochim. Acta 70, 2699–2714.
Nicholson, S.E., 2000. The nature of rainfall variability over Africa on time scales of decades to millenia. Global Planet. Change 26, 137–158.
Nicholson, S.E., Selato, J.C., 2000. The influence of La Niña on African rainfall. Int. J. Climatol. 20, 1761–1776.
Payne, B.R., 1970. Water balance of Lake Chala and its relation to groundwater from tritium and stable isotope data. J. Hydrol 11, 47–58.
Portielje, R., Lijkema, L., 1995. Carbon dioxide fluxes across the air-water interface and its impact on carbon availability in aquatic systems. Limnol. Oceanogr. 40, 690–699.
Rampen, S.W., Datema, M., Rodrigo-Gámiz, M., Schouten, S., Reichart, G.J., Sinninghe Damsté, J.S., 2014. Sources and proxy potential of long chain alkyl diols in lacustrine environments. Geochem. Cosmochim. Acta 144, 59–71.
Repeta, D.J., 1989. Carotenoid diagenesis in recent marine sediments: II. Degradation of fucoxanthin to loliolide. Geochem. Cosmochim. Acta 53, 699–707.
Rezanka, T., Podojil, M., 1986. Identification of wax esters of the fresh-water green alga *Chlorella kessleri* by gas chromatography-mass spectrometry. J. Chromatogr. 362, 399–406.
Rontani, J.F., Volkman, J.K., 2003. Phytol degradation products as biogeochemical tracers in aquatic environments. Org. Geochem. 34, 1–35.
Sachse, D., Billault, I., Bowen, G.J., Chikaraishi, Y., Dawson, T.E., Feakins, S.J., Freeman, K.H., Magill, C.R., McInerney, F.A., van der Meer, M.T.J., Polissar, P., Robins, R.J., Sachs, J.P., Schmidt, H.-L., Sessions, A.L., White, J.W.C., West, J.B., Kahmen, A., 2012. Molecular paleohydrology: interpreting the hydrogen-isotopic composition of lipid biomarkers from photosynthesizing organisms. Annu. Rev. Earth Planet Sci. 40, 221–249.
Schouten, S., Breteler, W.C.K., Blokker, P., Schogt, N., Rijpstra, W.I.C., Grice, K., Baas, M., Sinninghe Damsté, J.S., 1998. Biosynthetic effects on the stable carbon isotopic compositions of algal lipids: implications for deciphering the carbon isotopic biomarker record. Geochem. Cosmochim. Acta 62, 1397–1406.
Sinninghe Damsté, J.S., Verschuren, D., Ossebaar, J., Blokker, J., van Houten, R., van der Meer, M.T.J., Plessen, B., Schouten, S., 2011. A 25,000-year record of climate-induced changes in lowland vegetation of eastern equatorial Africa revealed by the stable carbon-isotopic composition of fossil plant leaf waxes. Earth Planet Sci. Lett. 302, 236–246.
Sinninghe Damsté, J.S., Ossebaar, J., Schouten, S., Verschuren, D., 2012. Distribution of tetraether lipids in the 25-ka sedimentary record of Lake Challa: extracting reliable TEX_{86} and MBT/CBT palaeotemperatures from an equatorial African lake. Quat. Sci. Rev. 50, 43–54.
Striegl, R.G., Kortelainen, P., Chanton, J.P., Wickland, K.P., Bugna, G.C., Rantakari, M., 2001. Carbon dioxide partial pressure and ^{13}C content of north temperate and boreal lakes at spring ice melt. Limnol. Oceanogr. 46, 941–945.
Tierney, J.E., Russell, J.M., Huang, Y., Sinninghe Damsté, J.S., Hopmans, E.C., Cohen, A.S., 2008. Northern Hemisphere controls on tropical Southeast African climate during the past 60,000 years. Science 322, 252–255.
Tierney, J.E., Mayes, M.T., Meyer, N., Johnson, C., Swarzenski, P.W., Cohen, A.S., Russell, J.M., 2010. Late-twentieth-century warming in lake Tanganyika unprecedented since AD 500. Nat. Geosci. 3, 422–425.
Tierney, J.E., Russell, J.M., Sinninghe Damsté, J.S., Huang, Y., Verschuren, D., 2011. Late quaternary behavior of the East African monsoon and the importance of the Congo air boundary. Quat. Sci. Rev. 30, 798–807.
Utermöhl, H., 1931. Neue Wege in der quantitativen Erfassung des Planktons. Verh. int. Ver. theor. angew. Limnol 5, 567–596.
Utermöhl, H., 1958. Zur vervollkommnung der quantitativen phytoplankton methodik. Mitt. Int. Ver. Theor. Angew. Limnol. 9, 1–38.
Verschuren, D., 2003. Lake-based climate reconstruction in Africa: progress and challenges. In: Aquatic Biodiversity. Springer, Dordrecht, pp. 315–330.
Verschuren, D., Russell, J.M., 2009. Paleolimnology of African lakes: beyond the exploration phase. PAGES News 17, 112–114.
Verschuren, D., Sinninge Damsté, J.S., Moernaut, J., Kristen, I., Blaauw, M., Fagot, M.,

Haug, G.H., CHALLACEA project members, 2009. Half-processional dynamics of monsoon rainfall near the East African Equator. Nature 462, 637–641.
Versteegh, G.J.M., Bosch, H.-J., de Leeuw, J.W., 1997. Potential palaeoenvironmental information of C_{24} to C_{36} mid-chain diols, keto-ols and mid-chain hydroxy fatty acids; a critical review. Org. Geochem. 27, 1–13.
Villanueva, L., Besseling, M., Rodrigo-Gámiz, M., Rampen, S., Verschuren, D., Sinninghe Damsté, J.S., 2014. Potential biological sources of long chain alkyl diols in a lacustrine system. Org. Geochem. 68, 27–30.
Volkman, J.K., Johns, R.B., Gillan, F.T., Perry, G.J., Bavor Jr., H.J., 1980. Microbial lipids of an intertidal sediment - I. Fatty acids and hydrocarbons. Geochem. Cosmochim. Acta 44, 1133–1143.
Volkman, J.K., Jeffrey, S.W., Nichols, P.D., Rogers, G.I., Garland, C.D., 1989. Fatty acid and lipid composition of 10 species of microalgae used in mariculture. J. Exp. Mar. Biol. Ecol. 128, 219–240.
Volkman, J.K., Barrett, S.M., Dunstan, G.A., Jeffrey, S.W., 1992. C_{30}–C_{32} alkyl diols and unsaturated alcohols in microalgae of the class Eustigmatophyceae. Org. Geochem. 18, 131–138.
Volkman, J.K., Barrett, S.M., Blackburn, S.I., Mansour, M.P., Sikes, E.L., Gelin, F., 1998. Microalgal biomarkers: a review of recent research developments. Org. Geochem. 29, 1163–1179.
Volkman, J.K., Barrett, S.M., Blackburn, S.I., 1999. Eustigmatophyte microalgae are potential sources of C_{29} sterols, C_{22}–C_{28} *n*-alcohols and C_{28}–C_{32} *n*-alkyl diols in freshwater environments. Org. Geochem. 30, 307–318.
Wanninkhof, R., Knox, M., 1996. Chemical enhancement of CO_2 exchange in natural waters. Limnol. Oceanogr. 41, 689–697.
Winters, K., Parker, P.L., van Baalen, C., 1969. Hydrocarbons of blue-green algae: geochemical significance. Science 163, 467–468.
Wolff, C., Haug, G.H., Timmermann, A., Sinninghe Damsté, J.S., Brauer, A., Sigman, D.M., Cane, M.A., Verschuren, D., 2011. Reduced interannual rainfall variability in East Africa during the last ice age. Science 333, 743–747.
Wolff, C., Kristen-Jenny, I., Schettler, G., Plessen, B., Meyer, H., Dulski, P., Naumann, R., Brauer, A., Verschuren, D., Haug, G.H., 2014. Modern seasonality in Lake Challa (Kenya/Tanzania) and its sedimentary documentation in recent lake sediments. Limnol. Oceanogr. 59, 1621–1636.